Received January 27, 2021, accepted January 29, 2021, date of publication February 2, 2021, date of current version February 10, 2021.
Digital Object Identifier 10.1109/ACCESS.2021.3056413

Synthetic Adaptive Fuzzy Disturbance Observer and Sliding-Mode Control for Chaos-Based Secure Communication Systems

VAN NAM GIAP [1], QUANG DICH NGUYEN [2], AND SHYH-CHOUR HUANG [1], (Senior Member, IEEE)
[1]Department of Mechanical Engineering, National Kaohsiung University of Science and Technology, Kaohsiung 807618, Taiwan
[2]Institute for Control Engineering and Automation, Hanoi University of Science and Technology, Hanoi 100000, Vietnam
Corresponding author: Shyh-Chour Huang (shuang@nkust.edu.tw)

This work was supported by the Ministry of Science and Technology of the Republic of China under Contract MOST 109-2622-E-992-008-CC3.

ABSTRACT This paper aims to present secure communication based on master and slave Lorenz chaotic systems. To apply a form of the linear synchronization control method, the mathematical models of master and slave systems were reformed into Takagi-Sugeno (T-S) fuzzy systems. First, the Lorenz chaotic system was completely changed to the form of the T-S fuzzy model with two sublinear systems and two boundary fuzzy membership functions. Second, a newly adaptive disturbance observer (ADOB) was proposed with a high convergent speed for the synchronization system, which was based on the basic nonlinear disturbance observer. Third, adaptive sliding-mode control (ASMC) has been constructed to synchronize the master and slave systems of a secure communication system. The stability of the proposed control algorithms was shown by solving the Lyapunov condition with the support of Young's inequality. The synchronization of two nonidentical chaotic Lorenz systems was utilized to encrypt and decrypt the data. Transmitted and decrypted signals are used to show that the proposed algorithms are adequate for the secure communication system. To confirm the originality and power of the proposed algorithms, secure communication between two computers was implemented perfectly through an internet router and electronic circuit communication scenarios.

INDEX TERMS Takagi-Sugeno fuzzy system, adaptive fuzzy disturbance observer, adaptive fuzzy sliding-mode control, secure communication system.

I. INTRODUCTION

In recent years, the 4.0 industrial revolution has taken over all manufacturing processes in the world. This is an opportunity for all of the new technology empires. However, this is also a challenge to all traditional technology firms. The key to the success of this revolution is the database, using which people can manage and control the manufacturing process easily and completely. Following this development, data secure communication is a requirement. Related to the field of data secure communication many papers proposed a solution to fulfill these requirements such as: Chen *et al.* [1], who proposed a secure communication system based on computers. Their paper introduced the H-infinity combined with sum-of-squares to synchronize and effectively reject disturbances. Çiçek *et al.* [2] proposed a new logic element chaotic system to provide a secure communication system background. Their sliding-mode control is an important portion of the synchronization algorithm. Their paper ignored the disturbance and uncertainty effects, where the resistors, capacitors, and wire coils are all nonlinear components. Delavari and Mohadeszadeh [3] proposed adaptive sliding-mode control for synchronizing the fractional-order hyperchaotic systems, where the adaptive sliding-mode control gains were obtained by applying the particle swarm optimization method. The decrypted signal was obtained as a precise copy of the transmitted signal. Vaseghi *et al.* [4] proposed an ASMC for secure communication in wireless sensor networks. Abd *et al.* [5] considered the delay time in data transmission with an adaptive observer to precisely synchronize the master

The associate editor coordinating the review of this manuscript and approving it for publication was Bing Li.

and slave systems. Chang *et al.* [6] revealed the secure communication of audio based on the field programmable gate array devices. The basic concept of secure communication based on a chaotic system is synchronization between the master and slave systems. Usually, the initial conditions of these systems are different. This leads to the master and slave system states being different from each other. To synchronize the signals between these systems, the control synchronization must be implemented correctly. Few papers in recent years have adequately presented the synchronization problem [7]–[10]. The application of synchronization for a network system has been investigated by papers [11]–[14]. The synchronization of memristive neural network systems was presented in [15], [16]. The synchronization of electronic circuits is found in [17]–[20]. The synchronization of digital and analog chaotic systems was discussed in [21], [22]. We recently proposed a new disturbance observer based on D-stability for synchronizing two non-identical T-S fuzzy chaotic systems. Two experimental cases of the proposed approach were well performed on computers with electronic circuit synchronization [23]. In previous papers [2], [3] and [48] there are no disturbance observers for the synchronization, which leads the performance of the real experiment synchronization system to go awry. In [2] sliding-mode control was proposed for synchronizing a chaotic logic system without the existence of disturbance. Their proposed control algorithm is good for simulation or only under certain ideal experimental conditions. In [3] the synchronization of a fractional-order system was investigated with the existence of disturbance, where the adaptive control was considered to synchronize and reject the disturbance. However, the performance described in the paper could be improved if the disturbance can be exactly compensated. In [48] output-feedback is considered to synchronize two chaotic systems. The disturbance observer was also ignored. There has been little discussion on the synchronization of chaotic systems to solve the deficiencies of previous papers. Motivated by the weak points of the number of adaptive disturbance observers and adaptive synchronization control, this paper proposes synthetic adaptive fuzzy disturbance observer and sliding-mode control. The proposed control algorithms include a new adaptive fuzzy disturbance observer and an ASMC linked together to gain the best synchronization precision. The observer and controller were designed based on the master and slave systems with the full advantages of T-S fuzzy control design. The observer and controller parameters can be obtained easily. A Takagi-Sugeno fuzzy system for master and slave is used to construct the controller and observer only. The systems for encryption and decryption the data still maintain in the form of Lorenz chaotic systems.

The T-S fuzzy system was investigated first in 1985 [24]. It is briefly represented by Tanaka and Wang [25]. Their study introduced the few methods of finding the T-S fuzzy mode by converting the original nonlinear mathematical mode into a combination of sublinear systems and fuzzy membership functions. The T-S fuzzy modeling method plays the role of nonlinear modeling with the sublinear systems and if-then rules. This role executes without loss of generality of the characteristics of the original system. The T-S fuzzy mode can take its advantages into the construction of a synchronized master and slave for chaotic systems in [26]–[32]. According to the author' best knowledge, investigations of the disturbance observer for synchronizing chaotic systems by application of T-S fuzzy systems implemented with actual experiments are minimal. In this work, the T-S fuzzy mathematical model was given by solving the sector nonlinearity due to its simple and intuitive nature. In the format of the T-S fuzzy model, the Lorenz system can be used to represent the ideas. The Lorenz system was invented by Lorenz in 1963 [33]. The system given by Lorenz with the butterfly effects of his work is an underlying concept of chaos theory, in which the states of the systems have sensitive initial conditions. The synchronization of the Lorenz system has been investigated in [17], [34]–[36]. This paper uses the two nonidentical chaotic Lorenz systems to do communication background. The states of the master and slave system are synchronized by adaptive fuzzy sliding-mode control. The effects of disturbance and variation in the system parameters on both systems can be completely deleted by an adaptive fuzzy disturbance observer. This method can be called the sump of synchronization disturbance rejection.

The disturbance observer has an important impact in control theory. It is well known as a special case of unknown input observer. To design a disturbance observer for a chaotic system is a complicated and expensive task. The disturbance observer for a chaotic system can easily be archived when the form of the chaotic system is converted to that of a T-S fuzzy system. Related to this problem, Selvaraj *et al.* [37] proposed the equivalent input disturbance-based repetitive for a T-S fuzzy system. Sakthivel *et al.* [38] proposed the disturbance and uncertainty rejection based on a low-pass-filter technique. Hwang and Kim [39] proposed a very effective extended disturbance observer-based integral sliding-mode control. However, the form of disturbance was assumed to be a specific form. These papers proposed the disturbance without a conjunction of control and disturbance. This paper proposes a new adaptive fuzzy disturbance to reject perturbation values of the synchronization systems. Our proposed method is based on the basic nonlinear disturbance observer, which was revealed by Chen [40]. The originality of our new observer is that the disturbance convergence is exponentially adaptive. However, the assumption that the derivative of the disturbance is located within a constant range is still helpful. Some applications of the basic nonlinear disturbance observer require the assumption that the first derivative of the disturbance is equal to zero [41]–[43]. To obtain an estimation of disturbance information, the ASMC could be introduced for synchronization control of master and slave Lorenz systems.

Sliding-mode control includes switching and equivalent control values. These values are used to force the system state to converge on a predefined surface and to stabilize the system state on that surface, respectively [44]. This kind of control can be considered as a nonlinear control algorithm with the main advantage of disturbance rejection ability. The problem of sliding-mode control is chattering, which occurs from the switching control part. Some improvements in freedom from chatter were introduced in [45]–[47]. Those papers discussed the concepts freedom from chatter through the witching control gains and boundary layer thickness of the saturation function in the switching control part. The adaptive law was newly constructed based on the error values of the system states. The convergence of proposed control method was proved by using the Lyapunov condition. Recent work [48] proposed feedback sliding-mode control and a norm observer connected in cascade to estimate the upper bound of the state variable for synchronizing unification of Lorenz and Chen systems. The achievements in those papers are benefit transmission the saw signal and the synchronization error values are small. However, some limitations still exists: The overshoot of the synchronization state response could be better, the settling time could improve faster, and the time required for the recovered signal to reach the original signal should be more improved. This paper aims to achieve smaller overshoots of synchronization errors, smaller settling times, and precise tracking between the received data and sent data. The main contributions and originality of the proposed methods are as follows:

1. In this paper, the Lorenz chaotic system was at a reduced scale, which was helpful for implementation of electronic circuit. Furthermore, to construct the disturbance observer for a secure communication system easily, the mathematical model of the Lorenz chaotic system was completely converted to the T-S fuzzy model. In our original study the T-S fuzzy model was only utilized for constructing the controller and observer. This meant that the master and slave systems were still maintained as Lorenz chaotic systems, as systems in (1) and (2). This work aims to reduce the cost of the experimental devices without loss of generality of master and slave system characteristics.
2. To reduce the problems of disturbance and uncertainty effects on the secure communication system, an adaptive fuzzy disturbance observer with new exponential gain was constructed to delete perturbation values of both sides of the master and slave systems. A main advantage of the proposed method is that the disturbance function gathers both the disturbance and uncertainty of the master and slave systems as one term. The gathered perturbation values can be deleted by a single disturbance observer, which is located on the slave system side.
3. To synchronize the master and slave systems, an adaptive fuzzy sliding-mode control was designed. The chattering of the sign function was deleted mostly by a simply adaptive law. The adaptive law was originated by integrating the absolute error of the synchronization state. The main chattering caused by switching control gain was minimized by a suitably adaptive gain.
4. To verify that the proposed control algorithms are corrected completely, they were implemented in a MATLAB simulation, computers communicated via an internet router, and experiments on the electronic circuits were performed.

The proposed control algorithms were used to solve the synchronization problem of two chaotic systems informing T-S fuzzy models. The first derivative of the disturbance is somehow deleted by the adaptive fuzzy sliding-mode control under the Lyapunov condition with the support of Young's inequality. Furthermore, the adaptive values are easily obtained by integrating the absolute tracking error values.

Remark 1: The MATLAB simulation and experiments are used to show that the effects of disturbance on both master and slave can be gathered and deleted by a single disturbance observer. The communications of the computers and electronic circuits are used to verify the proposed control algorithm.

This article is organized in the following manner: An introduction to trends in research, the proposed method concept, and its originality are given in the first section. The mathematical models of the system and problem description are given in the second part of the paper. Third, the synchronization algorithm and disturbance and uncertainty estimator are presented clearly in the third section. Fourth, an illustrative example of the study is given using MATLAB simulation, experiments in communication between computers via an internet router, and experiments on the electronic circuits. Finally, the conclusions and suggestions for future work are given.

Notations : $A > 0$ is a positively defined matrix. $A < 0$ is a negative defined matrix. I is the identity matrix. A^{-1} is the inverse matrix of A. If $s = [s_1 \ \ldots \ s_n]^T$ and $s \in R^n$ then $sign(s) = sign[s_1, \ldots, s_n]^T$, and $sign(s) = \frac{|s|}{s} = [\frac{|s_1|}{s_1} \ldots, \frac{|s_n|}{s_n}]^T$.

II. MATHEMATICAL MODELLING AND PROBLEM DISCRIPTION OF THE MASTER AND SLAVE SYSTEM

The Lorenz system presented in [33] can be rewritten with fully described disturbance and system parameter variation on three channels of the system as follows:

$$\begin{cases} \dot{x}_1(t) = (\delta + \Delta\delta)(x_2(t) - x_1(t)) + d_{x1}(t) \\ \dot{x}_2(t) = x_1(t)(\rho + \Delta\rho - x_3(t)) - x_2(t) + d_{x2}(t) \\ \dot{x}_3(t) = x_1(t)x_2(t) - (\beta + \Delta\beta)x_3(t) + d_{x3}(t) \end{cases} \quad (1)$$

where $x_1(t), x_2(t)$, and $x_3(t)$, are the system states: δ, ρ, and β are defined constants: $d_{x1}(t), d_{x2}(t)$, and $d_{x3}(t)$ are the disturbance values on $x_1(t), x_2(t)$, and $x_3(t)$, respectively. $\Delta\delta$, $\Delta\rho$, and $\Delta\beta$ are the system parameter variation values. The constant values of system (1) were selected as $\delta = 10$, $\rho = 28$, and $\beta = 8/3$. The system states of the system (1) were chosen out of the range $[-15; 15]$. The electronic circuit is not suitable illustrate chaotic characteristics. This paper modified the scale of the Lorenz system (1) without loss of the general characteristics of the original system. The modifications are $x_1(t) \rightarrow x(t)/10, x_2(t) \rightarrow y(t)/10$, and $x_3(t) \rightarrow z(t)/20$. System (1) can be written as follows:

$$\begin{cases} \dot{x}(t) = (\delta + \Delta\delta)(y(t) - x(t)) + d_x(t) \\ \dot{y}(t) = x(t)(\rho + \Delta\rho - 20z(t)) - y(t) + d_y(t) \\ \dot{z}(t) = 5x(t)y(t) - (\beta + \Delta\beta)z(t) + d_z(t) \end{cases} \tag{2}$$

The system state x is now a subset of $[-5; 5]$. System (2) can be converted into a new form as follows:

$$\begin{bmatrix} \dot{x}(t) \\ \dot{y}(t) \\ \dot{z}(t) \end{bmatrix} = \begin{bmatrix} -\delta_n + \Delta\delta & \delta_n + \Delta\delta & 0 \\ \rho_n + \Delta\rho & -1 & -20x(t) \\ 0 & 5x(t) & -\beta_n + \Delta\beta \end{bmatrix} \times \begin{bmatrix} x(t) \\ y(t) \\ z(t) \end{bmatrix} + \begin{bmatrix} d_x(t) \\ d_y(t) \\ d_z(t) \end{bmatrix} \tag{3}$$

Assumption 1: System (3) is warranted to work under outside and inside perturbations: these values of disturbance and uncertainty must be assumed to be bounded as follows: The disturbance values are bounded $|d_x(t)| < \xi_{dx}$, $|d_y(t)| < \xi_{dy}$, and $|d_z(t)| < \xi_{dz}$. The system parameter variations are bounded $|\Delta\delta| \leq \xi_\delta$, $|\Delta\rho| \leq \xi_\rho$, and $|\Delta\beta| \leq \xi_\beta$, respectively, where $\xi_{dx}, \xi_{dy}, \xi_{dz}, \xi_\delta, \xi_\rho$, and ξ_β are all positively defined.

Estimation of the disturbance term in system (1) is a complicated task. There are no physical sensors that can be used to measure these values directly. For this reason, the mathematical model could be suitably changed so that the disturbance observer/estimator can be applied to compensate the problem values. This paper uses T-S fuzzy mathematical modeling to build both the controller and observer. To give the reader a better understanding of the T-S fuzzy modeling method, the system is considered as follows:

$$\begin{cases} \dot{\chi}(t) = f^m(x(t), u(t))\chi(t) + g^m(x(t), u(t))\mathrm{u}(t) + d(t) \\ y(t) = h(x(t), u(t))\chi(t) \end{cases} \tag{4}$$

where f^m, g^m, and h^m are the smooth functions of the nonlinear system. System (4) can be converted to a T-S fuzzy model as follows:

$$\begin{cases} \dot{\chi}(t) = \sum_{i=1}^{r} \omega_i(\chi_i(t))\{(A_i\chi(t) + \Delta A_i\chi(t)) + (B_iu(t) \\ \qquad + \Delta B_iu(t)) + D_id(t)\} \\ y(t) = C\chi(t) \end{cases} \tag{5}$$

where $\chi(t) \in R^{n\times m}, u(t) \in R^{p\times m}$, and $y(t) \in R^{q\times m}$ are the system state, the control input, and the system output vectors, respectively. $d(t) \in R^{k\times m}$ is the disturbance. $A_i \in R^{n\times n}, B_i \in R^{n\times p}$, and $C \in R^{q\times n}$ are the state approximate matrices. $\Delta A_i \in R^{n\times n}$ is the uncertainty approximate of A and $\Delta B_i \in R^{n\times p}$ is the uncertainty approximate of B, respectively. $D_i \in R^{n\times k}$ is the approximate matrix of the disturbance. $\chi_i(t)$ is used as the membership values of the T-S fuzzy systems.

Assumption 2: The system (5) can work within some condition of the perturbations boundary as follows: The disturbance value is bounded $|D_id(t)| < \xi_d$, and the variation values are bounded $|\Delta A_i| \leq \xi_{\Delta Ai}$, and $|\Delta B_i| \leq \xi_{\Delta B_i}$, respectively. $\xi_d, \xi_{\Delta Ai}, \xi_{\Delta B_i}$ are all positively defined.

Assumption 3: To more easily obtain the disturbance and uncertainty without loss of generality of estimate these values separately, the assumption of a group of disturbances and uncertainty $\Delta A_ix(t) + \Delta B_iu(t) + D_id(t) = E_iL(t)$ is given where $E_i \in R^{3\times 3}$ a defined constant matrix, and $L(t) = [L_1(t),\ L_2(t),\ L_3(t)]^T$ is the lumped disturbance and uncertainty.

Remark 2: B_i and E_i should be selected as the identity matrices to more easily design the disturbance and uncertainty.

System (5) could be simplified as follows:

$$\begin{cases} \dot{\chi}(t) = \sum_{i=1}^{r} \omega_i(\chi_i(t))\{A_i\chi(t) + B_iu(t) + E_iL(t)\} \\ y(t) = C\chi(t) \end{cases} \tag{6}$$

The conversion of system (4) to (5) could be executed by applying the variable scheduling $\chi_i(t) \in [-\chi_{\min}(t), \chi_{\max}(t)]$. The weighting function of the T-S fuzzy modeling method is represented as follows:

$$\begin{cases} \omega_0^l(\chi_l) = \dfrac{\chi_{\max}^l - \chi_l(\cdot)}{\chi_{\max}^l - \chi_{\min}^l} \\ \omega_1^l(\chi_l) = 1 - \omega_0^l \end{cases} \tag{7}$$

where $\chi_{\max}^l$ is the maximum system state, and $\chi_{\min}^l$ is minimum system state; and $\omega_0^l(\chi_l)$ and $\omega_1^l(\chi_l)$ are the fuzzy membership functions for each variable function. System (3) consists of a single variable and the system then can be converted to the T-S fuzzy form as follows:

$$\begin{bmatrix} \dot{x}(t) \\ \dot{y}(t) \\ \dot{z}(t) \end{bmatrix} = \begin{bmatrix} -\delta_n + \Delta\delta & \delta_n + \Delta\delta & 0 \\ \rho_n + \Delta\rho & -1 & -20x(t) \\ 0 & 5x(t) & -\beta_n + \Delta\beta \end{bmatrix} \times \begin{bmatrix} x(t) \\ y(t) \\ z(t) \end{bmatrix} + \begin{bmatrix} d_x(t) \\ d_y(t) \\ d_z(t) \end{bmatrix} \tag{8}$$

By applying the T-S fuzzy modeling method with an operation of the sector nonlinearity rule, system (8) can be obtained as the mathematical model in the form of Eq. (6) with the system parameters defined as follows:

$$\omega_1(\theta(t)) = \frac{x_{\max} + x(t)}{x_{\max} - x_{\min}} \text{ and } \omega_2(\theta(t)) = \frac{x_{\max} - x(t)}{x_{\max} - x_{\min}}.$$

$$A_1 = \begin{bmatrix} -10 & 10 & 0 \\ 28 & -1 & -100 \\ 0 & 25 & 0 \end{bmatrix}, A_2 = \begin{bmatrix} -10 & 10 & 0 \\ 28 & -1 & 100 \\ 0 & -25 & 0 \end{bmatrix},$$

$$B_1 = \begin{bmatrix} 1 & 0 & 0 \\ 0 & 1 & 0 \\ 0 & 0 & 1 \end{bmatrix}, B_1 = B_2, E_1 = E_2 = \begin{bmatrix} 1 & 0 & 0 \\ 0 & 1 & 0 \\ 0 & 0 & 1 \end{bmatrix},$$

$$C = [1\ 0\ 0], \text{ and } x_i(t) \in [-5, 5].$$

The trajectory of the system states and its phase portraits of the Lorenz system with these above parameters and initial conditions of $\chi(0) = [0.1,\ 0.1,\ 0.1]^T$ are shown in Figure 1 below.

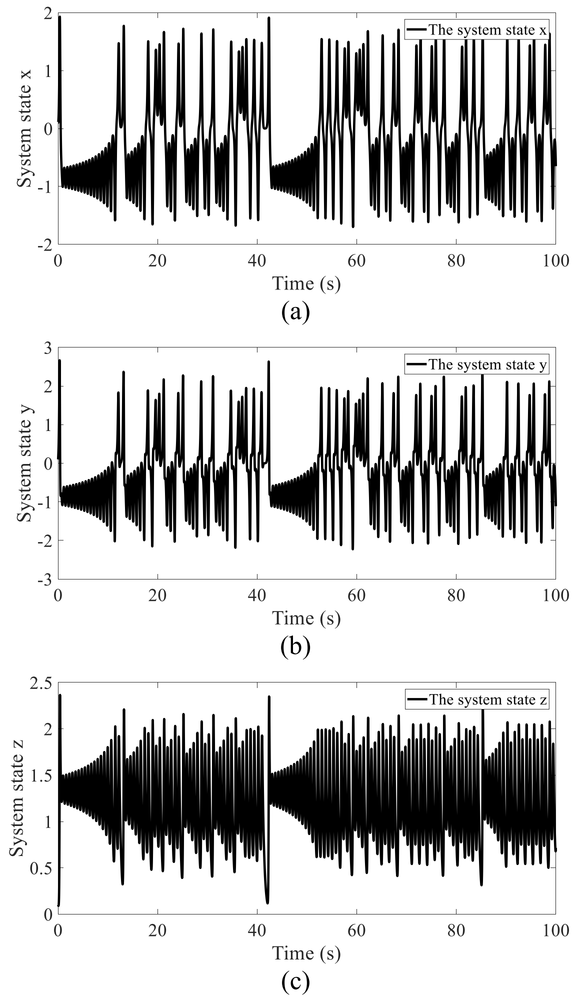

FIGURE 1. The rescaled Lorenz system states trajectories: (a) x-axis state value, (b) y-axis state value, (c) z-axis state value.

The system states show that the rescaled system does not lose the generality characteristics of chaotic phenomenon. The rescaled system states in Figure 1 are used to show that the Lorenz system is chaotic and nonperiodic. It is suitable for encryption and decryption of the data of secure communication applications. The phase portraits of the rescaled Lorenz system are shown as following Figure 2 below.

The system states phase portraits showed the conversion of the Lorenz system mathematical model without loss of generality. An ordinary differential equation with variable step size was used to simulate systems (2) and (3). To implement these Lorenz concepts in electronic circuit, time scaling is one of the most important factor after range of the states. The time scaling is an important factor for selecting the electronic components, and transferring the transmission signal, due to the device's frequency bandwidth, etc. To rescale the time

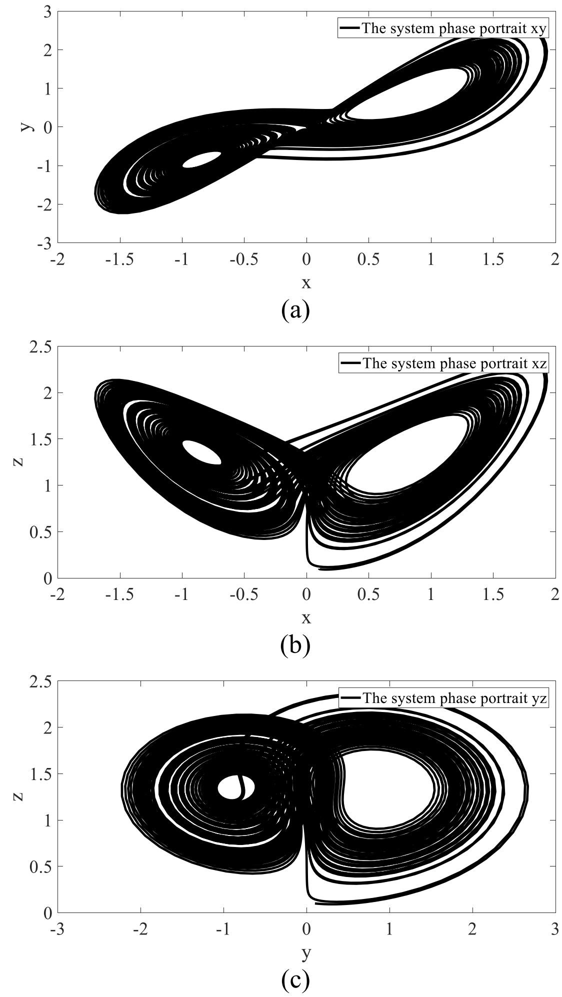

FIGURE 2. The rescaled Lorenz system phase portraits: (a) yx-axis phase trajectory, (b) zx-axis phase trajectory, and (c) zy-axis phase trajectory.

scales of the Lorenz chaotic system without the loss of generality characteristics, the capacitor and resistor values of the differential parts can be changed suitably. This paper reduced the time scale down 1000 times by changing the capacitors and resistor values. The initial values of the master and slave systems are can also be defined by these changes.

Remark 3: The MATLAB simulation and computer communication experiment scenarios used the rescaled state value systems. The electronic circuit communication used the system with rescaled states and times.

The system states and phase portraits are given in Figure 3 below.

The three system states in Figure 3 show that the electronics implementation is applicable without loss of the original characteristics of the Lorenz chaotic system in (1). For more details of the rescaled Lorenz system characteristics, the system phase trajectories are displayed in Figure 4 below to illustrate the rescaled Lorenz system behaviors.

By using the Lorenz system to illustrate the ideas of data secure communication due to its nonperiodic and chaotic behaviors, two nonidentical Lorenz systems were designed as

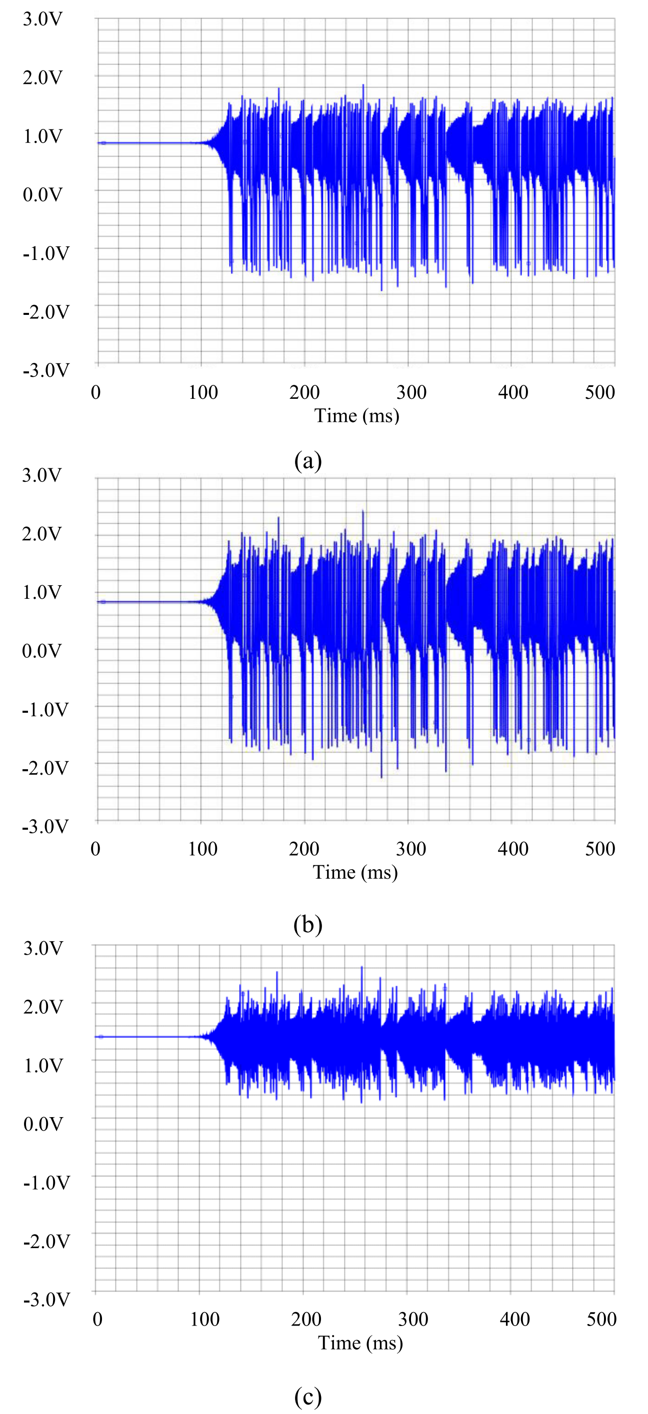

FIGURE 3. The Lorenz system states trajectories on a microsecond scale: (a) system state on x-axis, (b) system state on y-axis, (c) system state on z-axis.

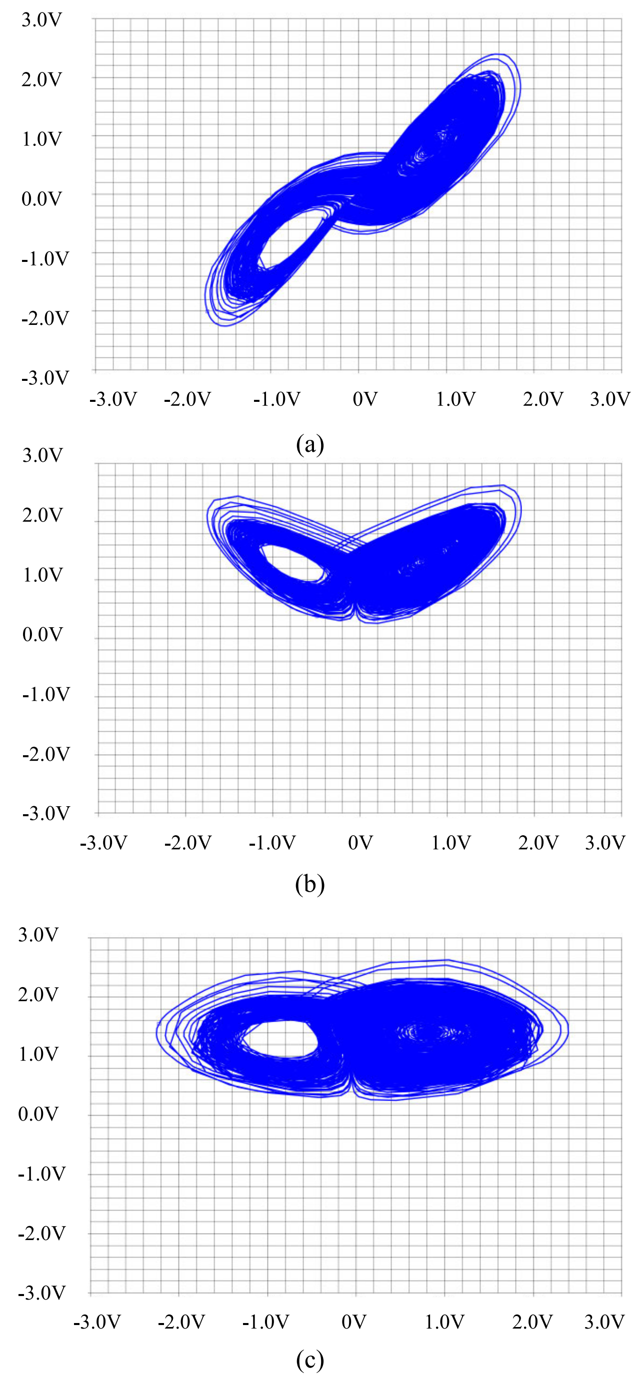

FIGURE 4. The Lorenz system states phase portraits on a microsecond scale: (a) yx-axis phase trajectory, (b) zx-axis phase trajectory, (c) zy-axis phase trajectory.

show in Figures 19 and 21 in the Appendix section. The initial conditions of the system can be represented by using different capacitor and resistor values for differential operations. To achieve precise signal transmission, the synchronization control must have qualified requirements. This paper uses the Lorenz system in the form of system (1) to construct the master and slave systems. The form of this system is described as follows:

$$\begin{cases} \dot{x}_m(t) = (\delta + \Delta\delta_m)(y_m(t) - x_m(t)) + d_{xm}(t) \\ \dot{y}_m(t) = x_m(t)(\rho_m + \Delta\rho_m - 20z_m(t)) - y_m(t) + d_{ym}(t) \\ \dot{z}_m(t) = 5x_m(t)y_m(t) - (\beta + \Delta\beta_m)z_m(t) + d_{zm}(t) \end{cases} \tag{9}$$

where m is used to represent the master term; $\Delta\delta_m$, $\Delta\rho_m$, and $\Delta\beta_m$ represent the parameter variations of the master system; and $d_{xm}(t)$, $d_{ym}(t)$, $d_{zm}(t)$ are disturbances of x-, y-, z-axis of the master system. All the system disturbances and uncertainty are assumed to fulfill assumption 1. System (9) can be converted into T-S fuzzy format in system (6) and represented as

$$\begin{cases} \dot{\chi}_m(t) = \sum_{i=1}^{r} \omega_i(x_m(t))\{A_i\chi_m(t) + E_iL_m(t)\} \\ y_m(t) = C\chi_m(t) \end{cases} \tag{10}$$

To obtain the precisely decrypted signal from the master transferred to the slave system, the control input could be introduced to the slave system. The slave system mathematical mode is then represented as follows:

$$\begin{cases} \dot{x}_s(t) = (\delta + \Delta\delta_s)(y_s(t) - x_s(t)) + d_{xs}(t) + u_{xs}(t) \\ \dot{y}_s(t) = x_s(t)(\rho_s + \Delta\rho_s - 20z_s(t)) - y_s(t) \\ \qquad +d_{ys}(t) + u_{ys}(t) \\ \dot{z}_s(t) = 5x_s(t)y_s(t) - (\beta + \Delta\beta_s)z_s(t) + d_{zs}(t) + u_{zs}(t) \end{cases} \tag{11}$$

where s is used to represent the slave term; $\Delta\delta_s$, $\Delta\rho_s$, and $\Delta\beta_s$ represent the parameter variations of the master system; and $d_{xs}(t)$, $d_{ys}(t)$, $d_{zs}(t)$ are disturbances of the x, y, z axis of the slave system, respectively. Disturbance and uncertainty values are assumed fulfill assumption 1. The conversion of the slave system into a T-S fuzzy system is shown as follows:

$$\begin{cases} \dot{\chi}_s(t) = \sum_{i=1}^{r} \omega_i(x_s(t))\{A_i\chi_s(t) + B_iu_s(t) + E_iL_s(t)\} \\ Y_s(t) = C\chi_s(t) \end{cases} \tag{12}$$

Remark 4: All the disturbances and system parameter variations of the master and slave systems have to fulfill assumptions 1 to 3. It is not possible to know exactly the disturbances and uncertainty boundaries. The term of lumped disturbance and uncertainty should accord with remark 1. The initial conditions of these systems are chosen differently.

The states error of master and slave systems is represented by

$$e = \chi_m - \chi_s \tag{13}$$

This paper used y_m and y_s to encrypt and decrypt the signal, respectively. By reference, the important signal before encryption is b_m and the signal after decryption is a_m. The requirement is that $a_m = b_m$ in all cases. The encrypted signal is $y_m + a_m$. The decrypted signal is

$$b_m = (y_m + a_m) - y_s \tag{14}$$

The precision transfer $a_m = b_m$ is fulfilled if the tracking error states of master and slave $e(t) \to 0$ as time proceeds to infinity. To obtain this goal, this paper proposed a synthetic adaptive fuzzy disturbance observer and sliding-mode control to synchronize the master and slave systems.

III. SYNTHETIC ADAPTIVE FUZZY DISTURBANCE OBSERVER AND SLIDING-MODE CONTROL FOR CHAOTIC SECURE COMMUNICATION SYSTEMS

This section presents the adaptive fuzzy disturbance observer and ASMC for synchronizing the states of two nonidentical chaotic systems. The structure of this section is as follows: (a) The adaptive fuzzy disturbance observer is briefly introduced with the previous problem and our contributions. (b) The ASMC with freedom from chatter is given. (c) A synchronization and stability analysis is represented to illustrate the effectiveness of the proposed method.

A. ADAPTIVE FUZZY DISTURBANCE OBSERVER

To estimate the perturbation values of a chaotic system is a complicated or expensive task and especially for the estimation of disturbance and uncertainty for a chaotic synchronization system. For softening the cost of estimation of the unwanted terms, this study proposed a fuzzy disturbance observer with a highly convergent speed, which was constructed based on the disturbance observer of Chen [40]. Chen proposed a basic nonlinear disturbance observer to estimate the disturbance of the continuous-time system as follows:

$$\dot{X}(t) = a_1X(t) + a_2u(t) + a_3d(t) \tag{15}$$

The disturbance was constructed as follows:

$$\begin{cases} \rho_1(t) = -L_da_3\rho_1(t) - L_d(a_1X(t) + a_2u(t) + a_3\rho_2(t)) \\ \rho_2(t) = L_dX(t) \\ \hat{d}(t) = \rho_1(t) + \rho_2(t) \end{cases} \tag{16}$$

The convergence of the disturbance error was proved as

$$\dot{\tilde{d}}(t) = \dot{d}(t) - L_da_3\tilde{d}(t) \tag{17}$$

The convergence speed was fixed as the term $\exp(-L_da_3)$. Furthermore, since it is requested that the first derivative of the unknown disturbance is goes to zero, this is a problem of the proposed nonlinear disturbance. Our paper [19] recently proposed a new disturbance observer without the assumption of $\dot{d}(t) = 0$. That disturbance observer perfectly archived it. This paper proposes a new form of disturbance without loss of originality without the assumption $\dot{d}(t) = 0$. However, $\dot{d}(t)$ is assumed to be located within a fixed range. This value can definitely be deleted by the adaptive sliding-mode control. The form of the new disturbance observer is as follows:

$$\begin{cases} \rho_1(t) = -L_da_3\rho_1(t) - L_d(a_1X(t) + a_2u(t) + a_3\rho_2(t)) \\ \rho_2(t) = L_dX(t) \\ \hat{d}(t) = \hat{\alpha}(t)(\rho_1(t) + \rho_2(t)) \end{cases} \tag{18}$$

Proof 1: Disturbance observer convergence.

The derivative of observed disturbance is

$$\begin{aligned} \dot{\hat{d}} &= \hat{\alpha}(t)(\dot{\rho}_1(t) + \dot{\rho}_2(t)) \\ &= \hat{\alpha}(t)(-L_da_3\rho_1(t) - L_d(a_1X + a_2u + a_3\rho_2(t)) + L_d\dot{X}(t)) \\ &= \hat{\alpha}(t)(-L_da_3\rho_1(t) - L_d(a_1X(t) + a_2u(t) \\ &\quad + a_3\rho_2(t)) + L_d(a_1X(t) + a_2u(t) + a_3d(t))) \end{aligned}$$

$$= \hat{\alpha}(t)\left(-L_d a_3(\rho_1(t)+\rho_2(t)) + L_d a_3 d(t)\right)$$
$$= \hat{\alpha}(t)\left(L_d a_3 \tilde{d}(t)\right) \tag{19}$$

or

$$\dot{\tilde{d}}(t) = \dot{d}(t) - \hat{\alpha}(t) L_d a_3 \tilde{d}(t) \tag{20}$$

Remark 5: If the sliding mode can delete the term $\dot{d}(t)$, the disturbance error will go to zero with exponential speed.

Applying the new disturbance observer to synchronization between the master and slave systems first requires a form of Eq. (15). This study uses the derivative of the error state between master and slave system to obtain the goals.

$$\begin{aligned}\dot{e}(t) &= \dot{\chi}_m(t) - \dot{\chi}_s(t)\\ &= \sum_{i=1}^{r}\omega_i(x_m(t))\{A_i\chi_m(t) + E_i L_m(t)\}\\ &\quad - \sum_{i=1}^{r}\omega_i(x_s(t))\{A_i\chi_s(t) + B_i u_s(t) + E_i L_s(t)\}\end{aligned} \tag{21}$$

where $E = E_1 = E_2$ leads $\sum_{i=1}^{r}\omega_i(x_m(t))E_i L_m(t) = EL_m(t)$ and $\sum_{i=1}^{r}\omega_i(x_s(t))E_i L_s(t) = EL_s(t)$, then Eq. (21) can be simplified as follows:

$$\begin{aligned}\dot{e}(t) &= \sum_{i=1}^{r}\omega_i(x_m(t))\{A_i\chi_m(t)\}\\ &\quad - \sum_{i=1}^{r}\omega_i(x_s(t))\{A_i\chi_s(t) + B_i u_s(t)\} + E\bar{L}(t)\end{aligned} \tag{22}$$

$E\bar{L}(t)$ is the total value of the perturbation values of both master and slave system.

Assumption 4: The synchronization system can work if the disturbance and uncertainty of each master and slave system are bounded or the total disturbance and uncertainty values of both master and slave system is assumed to be $\left|\dot{\bar{L}}(t)\right| \leq \Xi$.

Remark 6: The total disturbance and uncertainty values of both master and slave can be gathered together as one unique term, and its sum can be deleted by the disturbance observer. The observer should be designed on the slave side to calculate all disturbance and uncertainty values.

Remark 7: Nonidentical chaotic systems are used to represent two different chaotic systems.

By substituting Eq. (18) to model in Eq. (22), the adaptive fuzzy disturbance observer is represented as follows:

$$\begin{cases}\dot{p}(\mathrm{t}) = -L_d E p(\mathrm{t}) - L_d(\sum_{i=1}^{r}\omega_i(x_m(\mathrm{t}))A_i x_m(\mathrm{t}) -\\ \sum_{i=1}^{r}\omega_i(x_s(\mathrm{t}))A_i x_s(\mathrm{t}) - B_i u_s(\mathrm{t}) + Eq(\mathrm{t}))\\ q(\mathrm{t}) = L_d e(\mathrm{t})\\ \hat{\bar{L}}(\mathrm{t}) = \hat{\alpha}(\mathrm{t})\sum_{i=1}^{r}\omega_i(x_s(\mathrm{t}))(p(\mathrm{t}) + q(\mathrm{t}))\end{cases} \tag{23}$$

Taking the derivative of the sum of the disturbance yields

$$\begin{aligned}\dot{\hat{\bar{L}}}(\mathrm{t}) &= \hat{\alpha}(\mathrm{t})\sum_{i=1}^{r}\omega_i(x_s(\mathrm{t}))(\dot{p}(\mathrm{t}) + \dot{q}(\mathrm{t}))\\ &= \hat{\alpha}(\mathrm{t})\sum_{i=1}^{r}\omega_i(x_s(\mathrm{t}))\{-L_d E p(\mathrm{t})\\ &\quad -L_d(\sum_{i=1}^{r}\omega_i(x_m(\mathrm{t}))A_i x_m(\mathrm{t})\\ &\quad -\sum_{i=1}^{r}\omega_i(x_s(\mathrm{t}))A_i x_s(\mathrm{t}) - B_i u_s(\mathrm{t}) + Eq(\mathrm{t})) + L_d\dot{e}(\mathrm{t})\}\\ &= \hat{\alpha}(\mathrm{t})\sum_{i=1}^{r}\omega_i(x_s(\mathrm{t}))\{-L_d E(p(\mathrm{t}) + q(\mathrm{t}))\\ &\quad -L_d(\sum_{i=1}^{r}\omega_i(x_m(\mathrm{t}))A_i x_m(\mathrm{t}) - \sum_{i=1}^{r}\omega_i(x_s(\mathrm{t}))A_i x_s(\mathrm{t})\\ &\quad -B_i u_s(\mathrm{t}) + Eq(\mathrm{t})) + L_d\sum_{i=1}^{r}\omega_i(x_m(\mathrm{t}))A_i x_m(\mathrm{t})\\ &\quad -\sum_{i=1}^{r}\omega_i(x_s(\mathrm{t}))A_i x_s(\mathrm{t})\\ &\quad -L_d B_i u_s(\mathrm{t}) + L_d E\bar{L}(\mathrm{t})\}\end{aligned} \tag{24}$$

Since $\sum_{i=1}^{r}\omega_i(x_s(\mathrm{t})) = 1$ and $\sum_{i=1}^{r}\omega_i(x_m(\mathrm{t})) = 1$, Eq. (24) can be simplified as

$$\dot{\hat{\bar{L}}}(\mathrm{t}) = \hat{\alpha}(\mathrm{t})\sum_{i=1}^{r}\omega_i(x_s(\mathrm{t}))(-L_d E p(\mathrm{t}) - L_d E q(\mathrm{t}) + L_d E\bar{L}(\mathrm{t})) \tag{25}$$

or

$$\dot{\hat{\bar{L}}}(\mathrm{t}) = \hat{\alpha}(\mathrm{t})L_d E\sum_{i=1}^{r}\omega_i(x_s(\mathrm{t})\tilde{\bar{L}}(\mathrm{t}) \tag{26}$$

where $\tilde{\bar{L}}(t) = \bar{L}(t) - \hat{\bar{L}}(t)$ is the sum of the disturbance error value. Subtracting both sides of Eq. (26) by $\dot{\bar{L}}(t)$ leads to the derivative of the sum of the disturbance errors, yielding

$$\dot{\tilde{\bar{L}}}(t)(t) = \dot{\bar{L}}(t) - \hat{\alpha}(t)L_d E\sum_{i=1}^{r}\omega_i(x_s(t)\tilde{\bar{L}}(t) \tag{27}$$

The derivative value of the sum of the disturbance $\dot{\bar{L}}(t)$ can be softened mostly by using adaptive sliding-mode control. The disturbance observer can estimate the unknown perturbation values precisely when $\hat{\alpha}(t)L_d E$ is positively defined. The exponential convergence speed of the disturbance observer can be adaptively designed as follows:

$$\dot{\hat{\alpha}}(t) = \alpha_0\int_0^t |e_i(\tau)|\,d\tau \tag{28}$$

The stability condition is given in the final of this section.

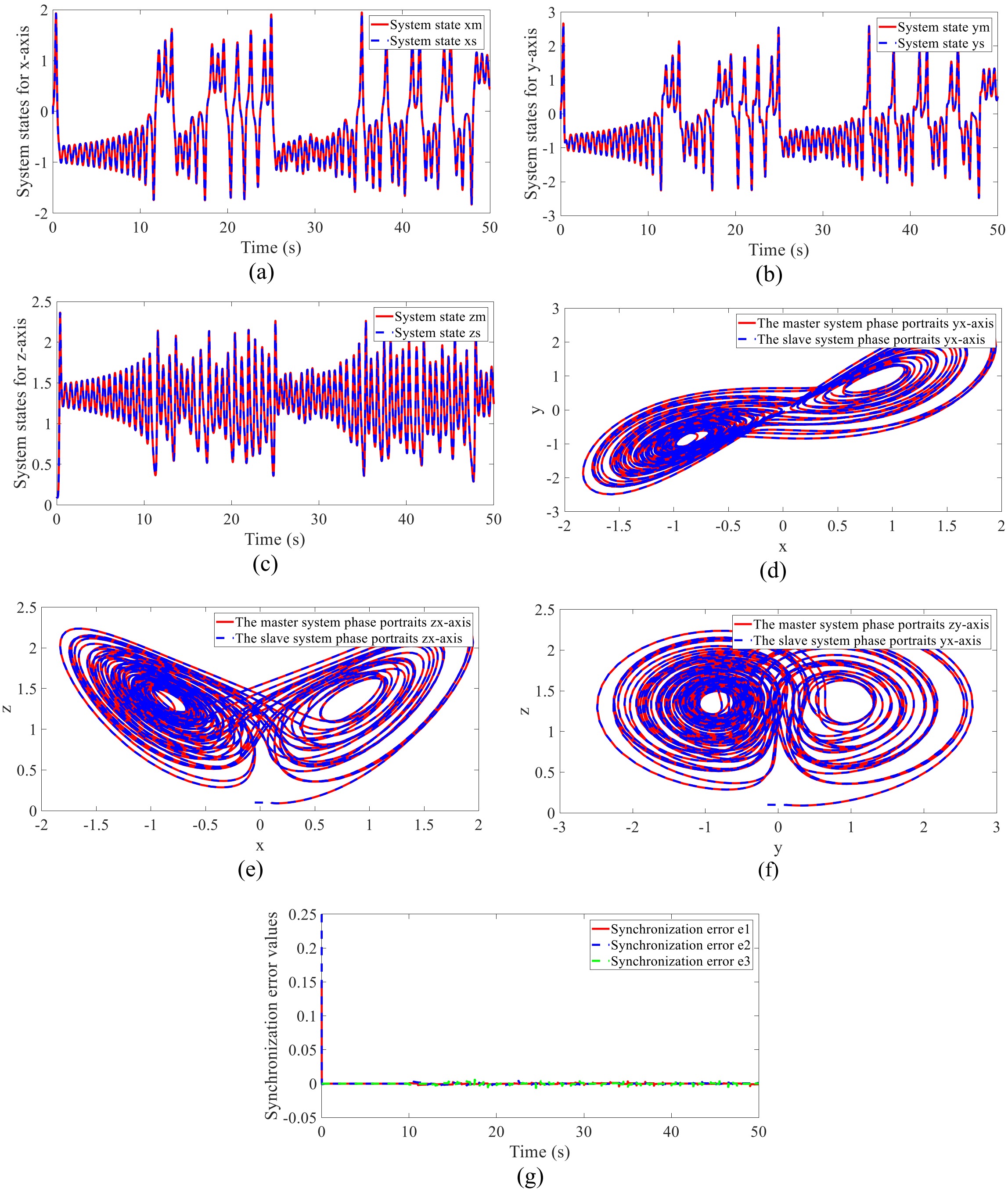

FIGURE 5. The synchronization output signals: (a) xm and xs signals, (b) ym and ys signals, (c) zm and zs signals, (d) yx-m and yx-s phase portraits, (e) zx-m and zx-s phase portraits, (f) zy-m and zy-s phase portraits, and (g) synchronization state error values.

B. ADAPTIVE FUZZY SLIDING-MODE CONTROL

To design sliding-mode control for synchronizing two non-identical chaotic systems is not complicated task. However, to design a disturbance observer for this operation is not so simple. This paper proposes a new adaptive fuzzy disturbance observer for estimating disturbance and uncertainty values of synchronization chaotic systems following the T-S fuzzy model control design. At this point, the sliding-mode control can be easily provided. Furthermore, the problem of sliding-mode chattering will be softened by an adaptive law. The sliding-mode surface is proposed as follows:

$$s(t) = e(t) + \lambda \int_{0}^{t} e(\tau)d\tau \tag{29}$$

Taking the first derivative of Eq. (29) yields

$$\dot{s}(t) = \dot{e}(t) + \lambda e(t) \tag{30}$$

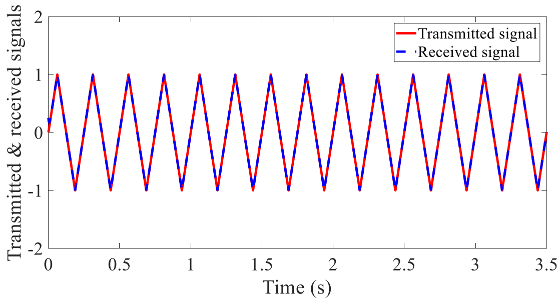

FIGURE 6. Transmitted and received data of secure communication between two nonidentical Lorenz systems in the first 3.5 seconds.

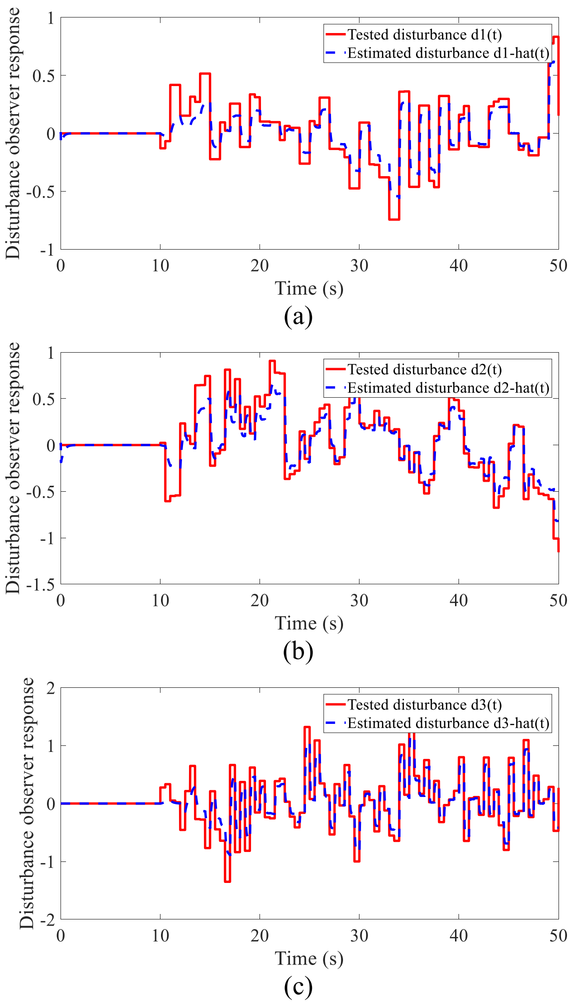

FIGURE 7. Tested and estimated disturbance on both master and slave Lorenz systems: (a) tested and estimated disturbance signals on x-axis, (b) tested and estimated disturbance signals on y-axis, (c) tested and estimated disturbance signals on z-axis.

Substituting Eqs. (13) and (22) into Eq. (30) with the feedback of the disturbance observer leads to

$$\dot{s}(t) = \sum_{i=1}^{r} \omega_i(x_m(t))\{A_i\chi_m(t)\}$$
$$-\sum_{i=1}^{r} \omega_i(x_s(t))\{A_i\chi_s(t) + B_i u_s(t)\} + E\tilde{\tilde{L}}(t) + \lambda e(t) \quad (31)$$

TABLE 1. The outcomes of our paper and paper [48].

Values	OUR PAPER RESULT	PAPER [48]
* *Overshoot*	Maximum value is $8.7\cdot10^{-4}$.	All values are out of the range of [-1;1]
* *Settling time*	0.03 (second)	After 1 (second)
* *States errors*	The range of 10^{-3}	Larger than scale of 10^{-3}
* *Background*	Simulation	Simulation

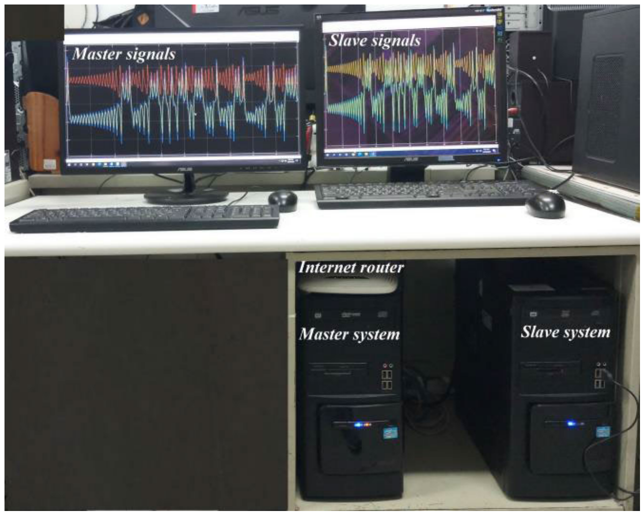

FIGURE 8. The experimental setup of computer communication.

Solving Eq. (31) by considering $\dot{s}(t) = 0$ can produce the equivalent control value as follows:

$$u_{eqs}(t) = [B_i^T B_i]^{-1} B^T \left\{ \sum_{i=1}^{r} \omega_i(x_m(t))\{A_i\chi_m(t)\} + E\tilde{\tilde{L}}(t) + \lambda e(t) - \sum_{i=1}^{r} \omega_i(x_s(t))\{A_i\chi_s(t)\} \right\} \quad (32)$$

where *eqs* refers to the equivalent control value of the sliding-mode control. This paper selected the switching control value to be as simple as possible for implementation in the electronic circuit. That is, the switching control is just about a sinusoidal function. However, to improve the precision of tracking between master and slave system states, adaptive switching control is designed. The switching control value was also given as follows:

$$u_{sws}(t) = -[B_i^T B_i]^{-1} B^T \hat{k}(t) sign(s(t)) \quad (33)$$

The word *sws* is used to represent the switching control for slave system. The fuzzy sliding-mode control is constructed by using fuzzy membership functions of the T-S fuzzy master and slave system states.

Definition 1: sign$(\cdot)$ is a signum function with

$$sig(\gamma) = \begin{cases} 1 & if \quad \gamma > 0 \\ 0 & if \quad \gamma = 0 \\ -1 & if \quad \gamma < 0 \end{cases} \quad (34)$$

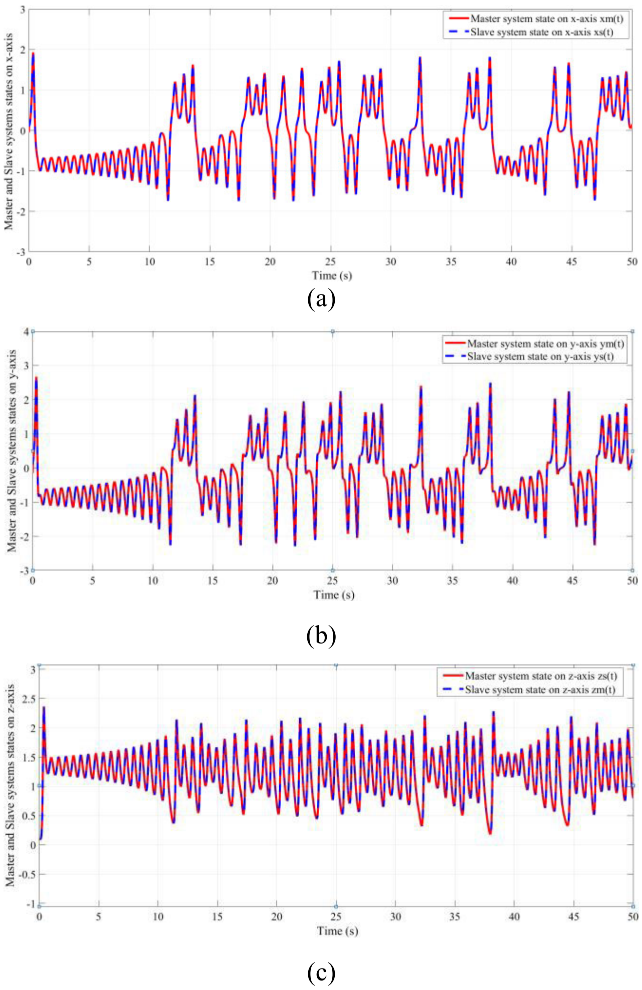

FIGURE 9. **The synchronization output signals: (a) xm and xs signals, (b) ym and ys signals, (c) zm and zs signals.**

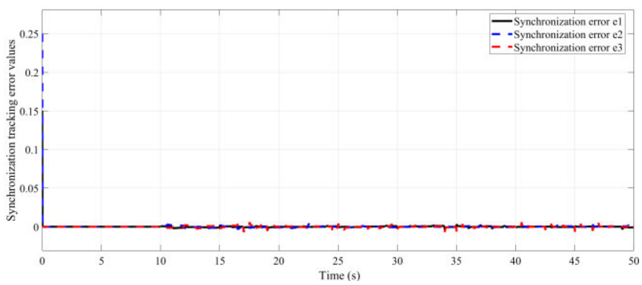

FIGURE 10. **The synchronization states' error for x-, y-, and z-axis.**

Basically, chattering comes from the switching control gains and in the boundary layer thickness of the switching control functions. This paper used the *sign* function to construct the switching control value. Chattering will be reduced significantly by the adaptive control as follows:

$$\dot{\hat{k}}(t) = k_0 \int_0^t |e_i(\tau)|\, d\tau \tag{35}$$

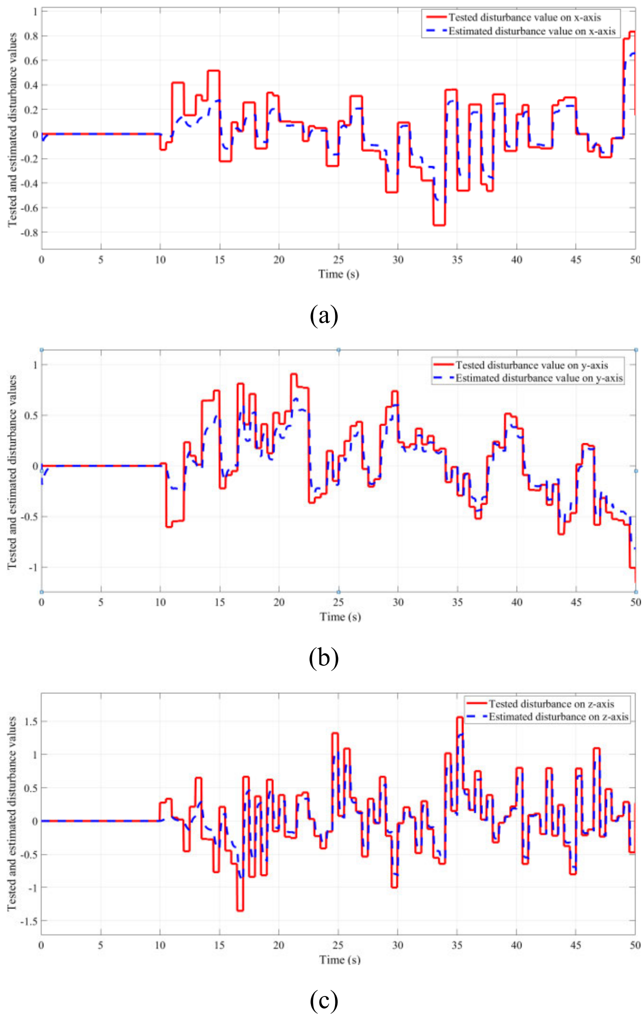

FIGURE 11. **Tested and estimated disturbance on both master and slave systems: (a) tested and estimated disturbance on x-axis, (b) tested and estimated disturbance on y-axis, and (c) tested and estimated disturbance on z-axis.**

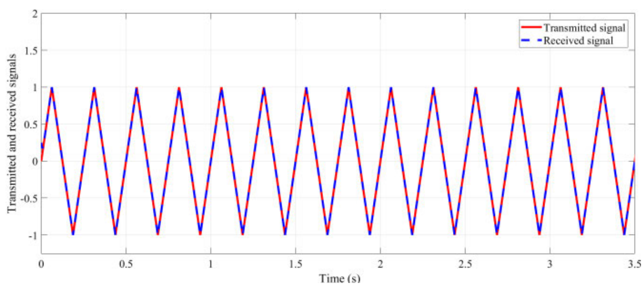

FIGURE 12. **Transmitted and received signals in first 3.5 second.**

The effectiveness of the proposed control method is given in the following section.

Lemma 1: Young's inequality: if a, b, m and n are all defined as positive real numbers and fulfill $\frac{1}{a} + \frac{1}{b} = 1$, then

$$m \cdot n \leq \frac{1}{a} m^a + \frac{1}{b} n^b. \tag{36}$$

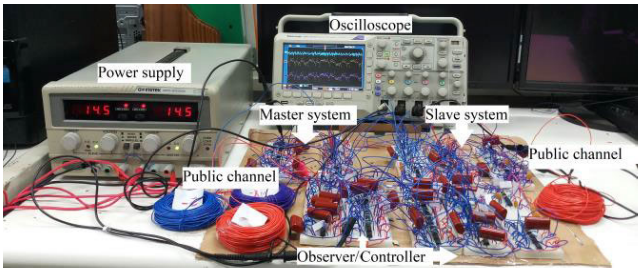

FIGURE 13. **Secure communication system based on electronic circuit design.**

C. STABILITY OF SYNCHRONIZATION CONTROL ANALYSIS

To confirm that the control and observer are truly necessary to the data secure communication systems, the synchronization must be fulfilled with the slave system states precisely tracking the master system trajectories. The necessary condition of convergence is given by combining the sliding-mode control and disturbance observer feedback.

$$\dot{e}(t) = \sum_{i=1}^{r} \omega_i(x_m(t))\{A_i\chi_m(t)\} - \sum_{i=1}^{r} \omega_i(x_s(t))\{A_i\chi_s(t) + B_i[[B_i^T B_i]^{-1}B^T\{\sum_{i=1}^{r} \omega_i(x_s(t))\{A_i\chi_s(t)\} - E\tilde{\tilde{L}}(t) - \lambda e(t) - \sum_{i=1}^{r} \omega_i(x_m(t))\{A_i\chi_m(t)\}\}\}] + E\tilde{\tilde{L}}(t) \quad (37)$$

or

$$\dot{e}(t) = -\lambda e(t) \quad (38)$$

The sufficient condition of the stability is when the sliding-mode gain λ is positively defined. With $\lambda > 0$, distance tracking error values of the master and slave system exponentially converge to zero in infinite time. The sufficient condition of convergence can be selected as

$$V(t) = \frac{1}{2}s^T(t)s(t) + \frac{1}{2}\tilde{\alpha}^T(t)\tilde{\alpha}(t) + \frac{1}{2}\tilde{k}^T(t)\tilde{k}(t) + |s(t)|\frac{1}{2}\tilde{\tilde{L}}^T(t)\tilde{\tilde{L}}(t) \quad (39)$$

Taking the derivative of Eq. (39) yields

$$\dot{V}(t) = s^T(t)\dot{s}(t) - \tilde{\alpha}^T(t)\dot{\hat{\alpha}}(t) - \tilde{k}^T(t)\dot{\hat{k}}(t) + |s(t)|\tilde{\tilde{L}}^T(t)\dot{\tilde{\tilde{L}}}(t)(t) \quad (40)$$

By using the combination of Eqs. 28, 30, 32, 33, and 35 to solve Eq. (40) leads to

$$\dot{V}(t) = s^T(t)(-\hat{k}(t)sign(s(t))) - \tilde{\alpha}^T(t)\dot{\hat{\alpha}}(t) - \tilde{k}^T(t)\dot{\hat{k}}(t) + |s(t)|\tilde{\tilde{L}}^T(t)[\dot{\tilde{L}}(t) - \hat{\alpha}(t)L_dE\sum_{i=1}^{r}\omega_i(x_s(t)\tilde{\tilde{L}}(t)] \quad (41)$$

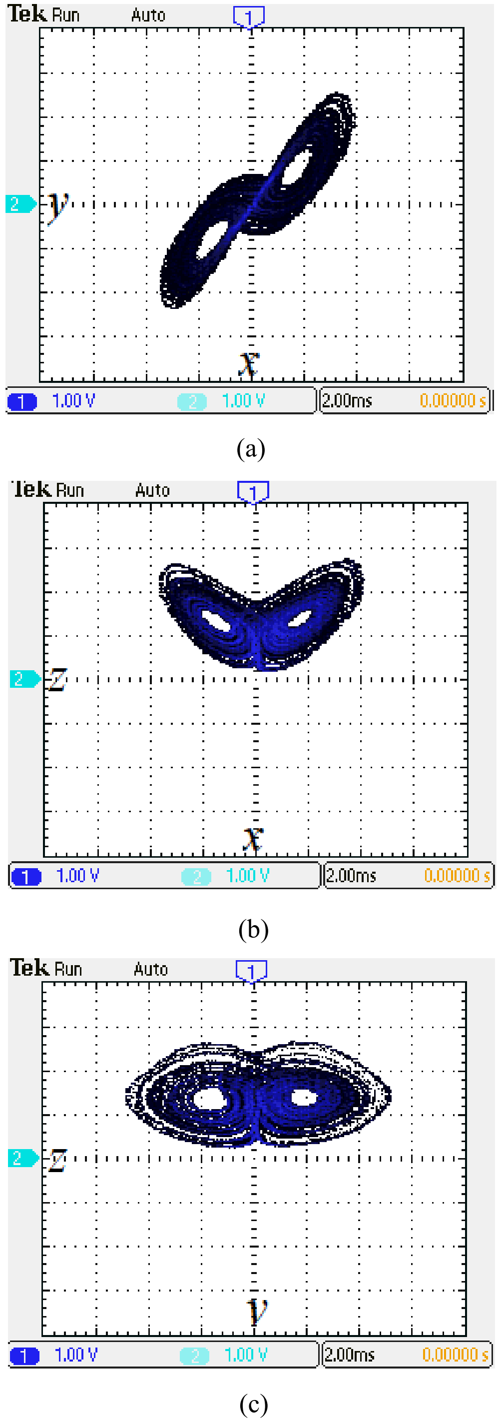

FIGURE 14. **Chaotic Lorenz system behavior: (a) y-x phase trajectory, (b) z-x phase trajectory, z-y phase trajectory.**

or

$$\dot{V}(t) = -\hat{k}(t)|s(t)| - \tilde{\alpha}^T(t)\alpha_0\int_0^t |e(\tau)|\,d\tau - \tilde{k}^T(t)k_0 \times \int_0^t |e(\tau)|\,d\tau + |s(t)|\tilde{\tilde{L}}^T(t)[\dot{\tilde{L}}(t) - \hat{\alpha}(t)L_dE$$

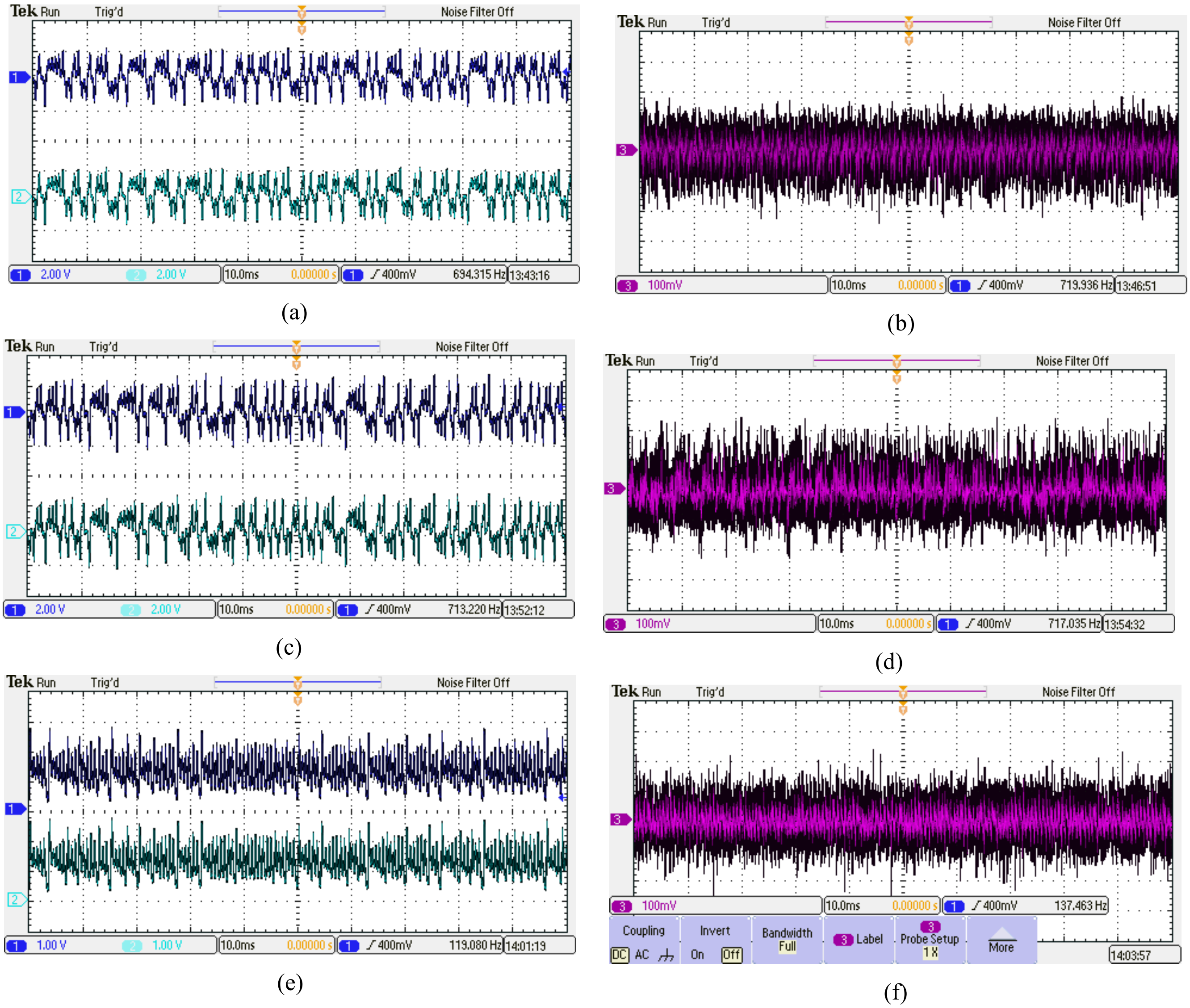

FIGURE 15. **Synchronization of electronic circuit implementation: (a) xm and xs signals, (b) tracking error value e1, (c) ym and ys signals, (d) tracking error value e2, (e) zm and zs signals, and (f) tracking error value e3.**

$$\times \sum_{i=1}^{r} \omega_i(x_s(t)\tilde{\bar{L}}(t)] \leq -\hat{k}(t)\,|s(t)| - \left|\tilde{\alpha}^T(t)\right| \alpha_0 \times \int_0^t |e(\tau)|\,d\tau - \left|\tilde{k}^T(t)\right| k_0 \int_0^t |e(\tau)|\,d\tau + |s(t)| \left|\tilde{\bar{L}}(t)\right| [\dot{\bar{L}}(t) - \hat{\alpha}(t)L_d E] \quad (42)$$

Applying lemma 1 and assumption 4 to Eq. (42) yields

$$\dot{V}(t) \leq -\hat{k}(t)\,|s(t)| - \left|\tilde{\alpha}^T(t)\right| \alpha_0 \int_0^t |e(\tau)|\,d\tau - \left|\tilde{k}^T(t)\right| k_0 \times \int_0^t |e(\tau)|\,d\tau + |s(t)|\,[\frac{1}{2}\left|\tilde{\bar{L}}(t)\right|^2 + \frac{1}{2}\Xi^2] - |s(t)|\,\hat{\alpha}(t)L_d E \left|\tilde{\bar{L}}(t)\right| \quad (43)$$

Eq. (43) can be simplified as follows:

$$\dot{V}(t) \leq |s(t)|\,[-\hat{k}(t) + \frac{1}{2}\left|\tilde{\bar{L}}(t)\right|^2 + \frac{1}{2}\Xi^2] - \left|\tilde{\alpha}^T(t)\right| \alpha_0 \times \int_0^t |e(\tau)|\,d\tau - \left|\tilde{k}^T(t)\right| k_0 \int_0^t |e(\tau)|\,d\tau - |s(t)|\,\hat{\alpha}(t)L_d E \left|\tilde{\bar{L}}(t)\right| \quad (44)$$

Inequality (44) satisfies $\dot{V}(t) < 0$ if $\alpha_0 > 0, k_0 > 0$, and $\hat{k}(t) \geq \frac{1}{2}\left|\tilde{\bar{L}}(t)\right|^2 + \frac{1}{2}\Xi^2$.

The proposed controller and observer for synchronizing two nonidentical chaotic Lorenz systems has been implemented through simulation and experiments. First,

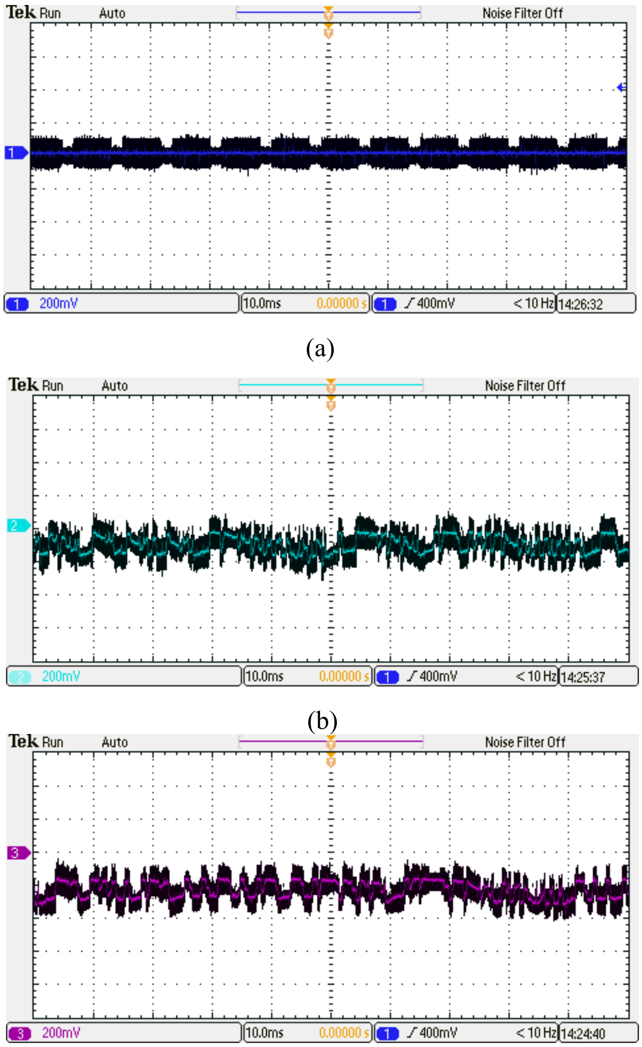

(a)

(b)

(c)

FIGURE 16. Disturbance and uncertainty values. (a) estimated disturbance on x-axis, (b) estimated disturbance on y-axis, and estimated disturbance on z-axis.

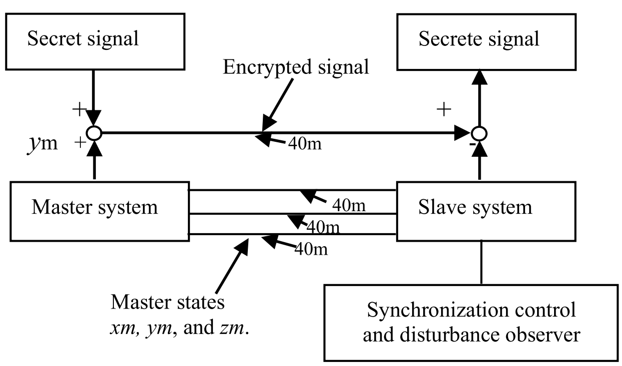

FIGURE 17. Data transmission structure.

the proposed method is simulated in MATLAB software. Second, these concepts were experimentally implemented using computer communication via an internet router and electronic circuits. The details are given in the following section.

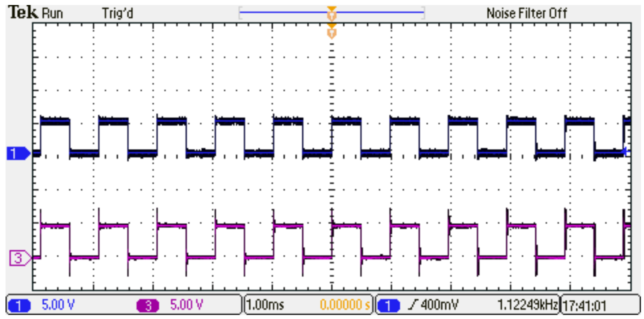

FIGURE 18. The original secret signal and its decrypted signal.

IV. ILLUSTRATIVE EXAMPLES

Basically, data secure communication can be successfully archived based on the precision of the synchronization between master and slave systems. The precision of synchronization is based on the control synchronization and disturbance rejection. This section presents the synchronization and data secure communication of two nonidentical chaotic Lorenz systems by using MATLAB simulation, computer communication, and implementation of electronic circuit. There are three cases in this study with the same systems, controller, and observer. The parameters of controller/observer for the MATLAB simulation and experiment were identical. These parameters differ from those used in the implementation of the electronic circuit. The MATLAB simulation and experiment are given with the aim that the tested disturbance to both master and slave systems can be deleted together by the adaptive fuzzy disturbance observer. Third, the synchronization of two nonidentical chaotic Lorenz systems was implemented on the electronic circuit as shown in Figures 19 to 25 in the Appendix. Otherwise, a distant square wave signal can be transmitted securely to the slave system.

A. SYNCHRONIZATION AND ITS APPLICATION OF TWO LORENZ CHAOTIC SYSTEMS BASED ON MATLAB SIMULATION

The initial state of the master system is $\chi_m(0) = [0.1,\ 0.1,\ 0.1]^T$. The initial conditions of the slave system are $\chi_s(0) = [-0.05,\ -0.15,\ 0.1]^T$. The control gains were selected as

$$\lambda = \begin{bmatrix} 200 & 0 & 0 \\ 0 & 200 & 0 \\ 0 & 0 & 200 \end{bmatrix},\ k_0 = \begin{bmatrix} 0.01 & 0 & 0 \\ 0 & 0.01 & 0 \\ 0 & 0 & 0.01 \end{bmatrix},$$

$$L_d = \begin{bmatrix} 4 & 0 & 0 \\ 0 & 3 & 0 \\ 0 & 0 & 4 \end{bmatrix},\ \text{and}\ \alpha_0 = \begin{bmatrix} 100 & 0 & 0 \\ 0 & 100 & 0 \\ 0 & 0 & 100 \end{bmatrix}.$$

due to the total disturbances on both systems being considered as a unique term of disturbance. The disturbance observer effectiveness will affect the system state behavior. However, there is a very small effect on the outcome of the control synchronization system. The characteristic of

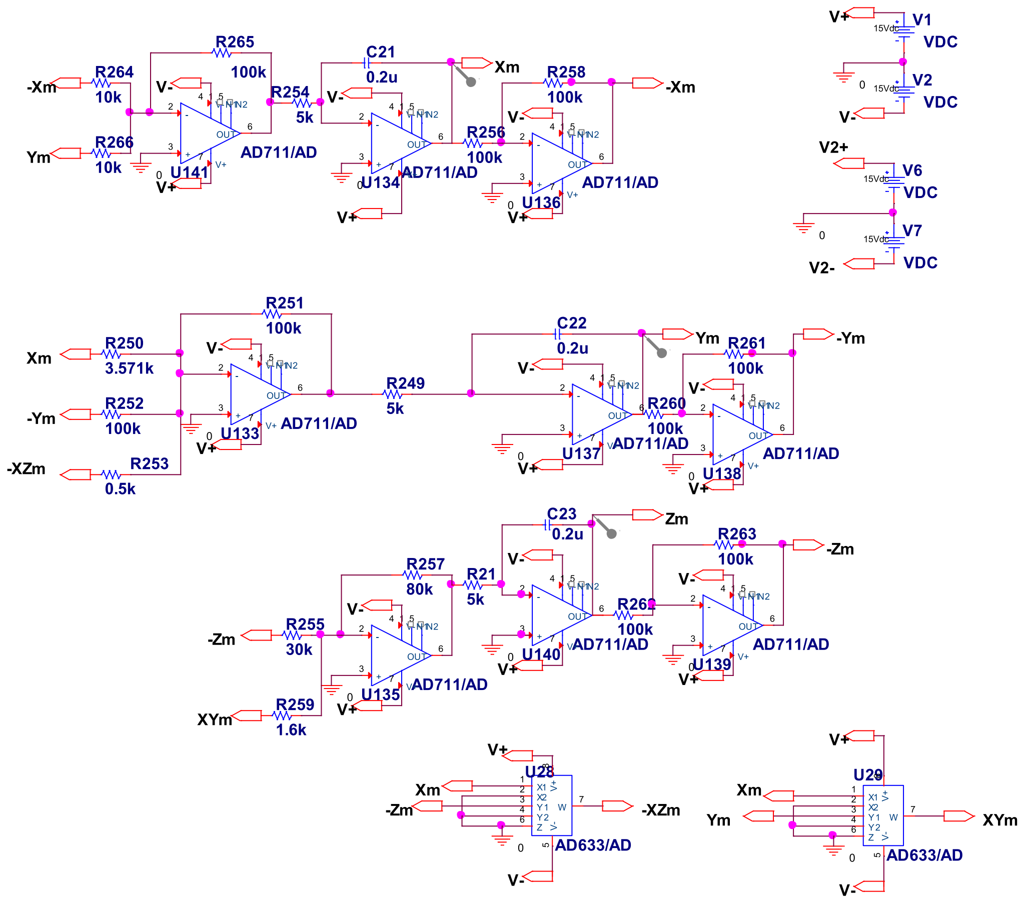

FIGURE 19. Master system circuit.

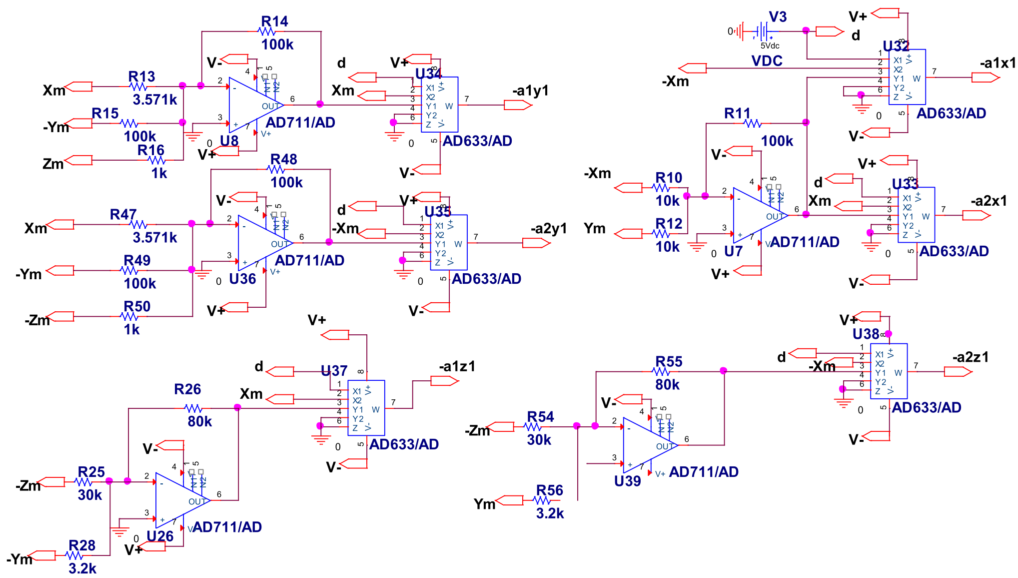

FIGURE 20. T-S fuzzy system calculation of master system.

two nonidentical systems are still completely maintained. The synchronization results are given in Figure 5 below.

To show the effectiveness of the proposed controller and observer, the synchronization was used to encrypt and decrypt

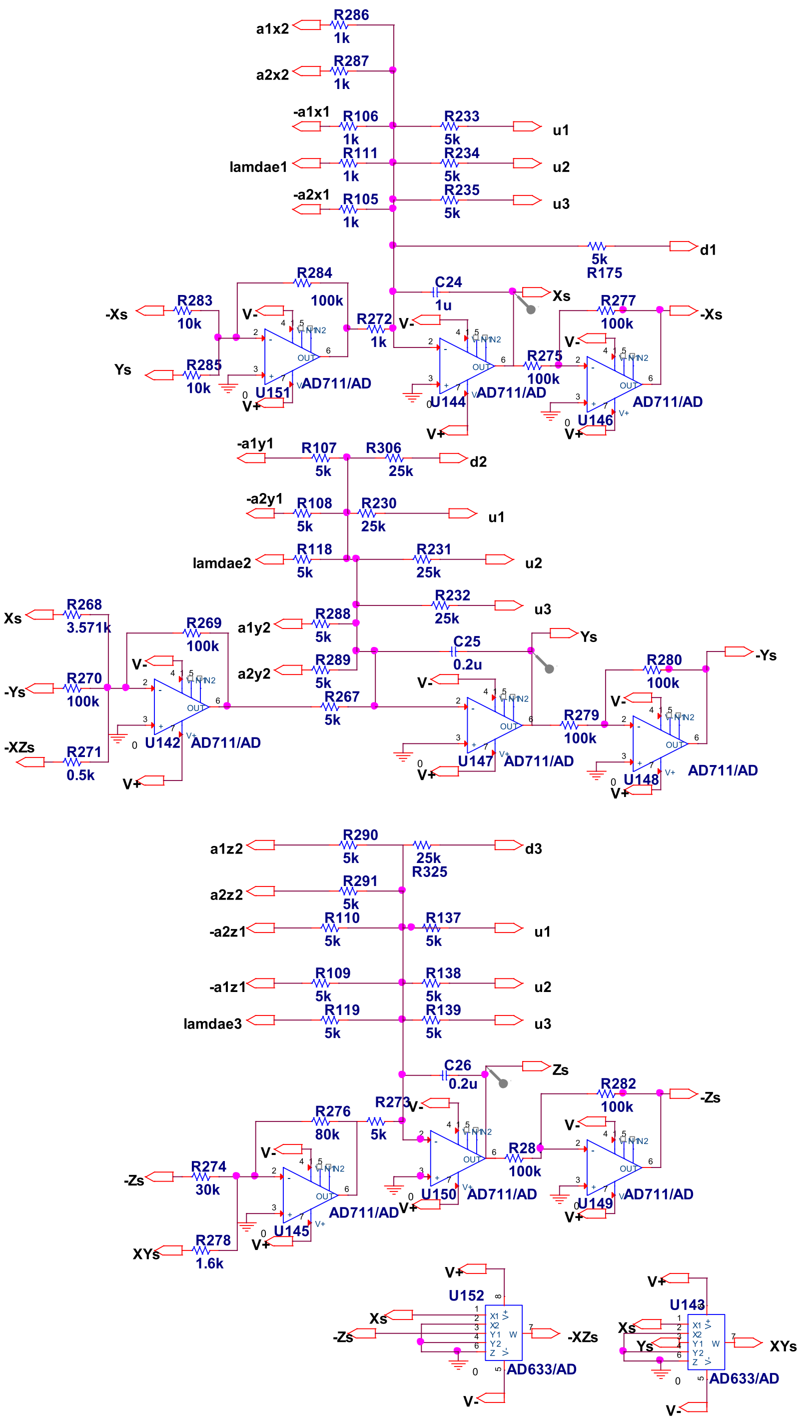

FIGURE 21. **Slave system in form of chaos system with support of controller and observer.**

the saw wave data. The data transmission is fulfilled as shown in Eq. (14), achieved as in Figure. 6 below.

The received data tracked the sent data very precisely. The observer responses to the tested disturbance in both master and slave systems are shown in Figure 7 below.

The tested disturbance on both master and slave systems were mostly estimated. The master and slave systems states precisely tracked each other with tracking error values of $e_1 \in [-4.14 \cdot 10^{-3}; 3.34 \cdot 10^{-3}]$, $e_2 \in [-3.82 \cdot 10^{-3}; 4.24 \cdot 10^{-3}]$ and $e_3 \in [-7.14 \cdot 10^{-3}; 6.00 \cdot 10^{-3}]$ for master and slave synchronization error on the x-, y-, and z-axis, respectively. The maximum reaching time approximately 0.03 second with no overshoot values. The estimated disturbance signals tracked the tested disturbance precisely, and the precision is increased

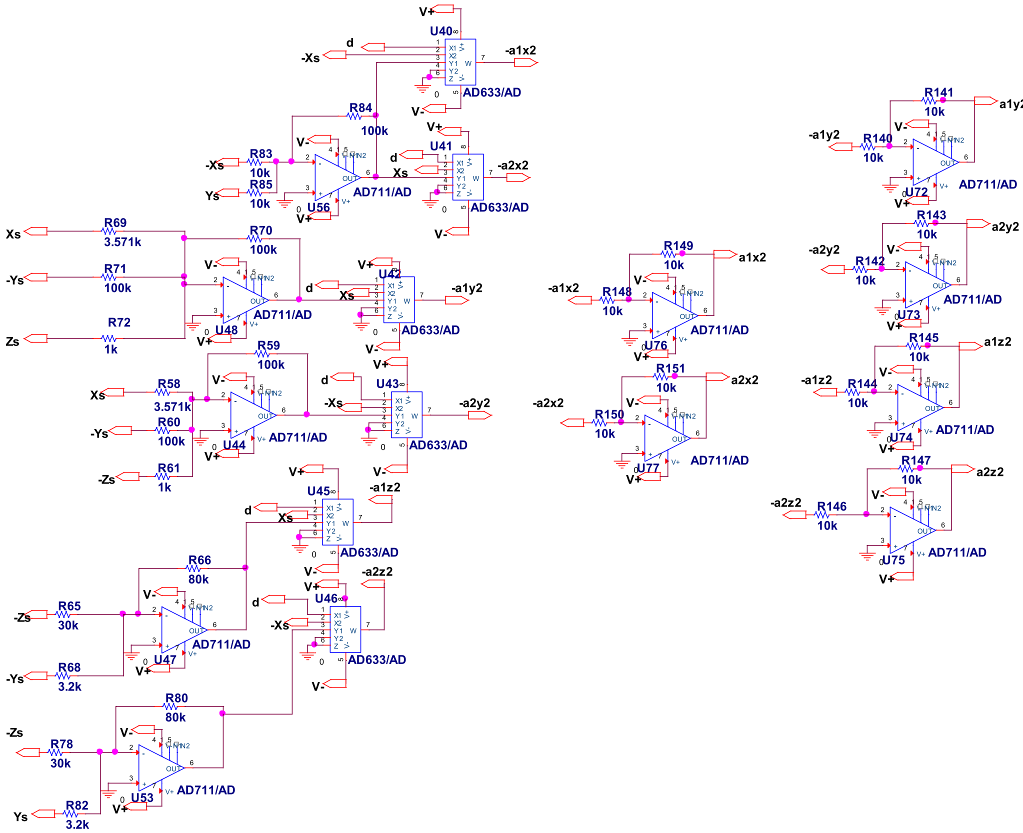

FIGURE 22. T-S fuzzy system calculation of slave system.

as time goes to infinity. The outcomes in this paper could be used to compare with those in a previous paper [48] to emphasize the effectiveness of the proposed algorithms. The comparison is shown in following Table 1 below.

The simulation of the proposed algorithms performed well when synchronizing the master and slave systems. The Lorenz chaotic system is retained for constructing master and slave mathematical models. In these systems the T-S fuzzy mode was used only for design of the controller and observer. The proposed algorithms are introduced to computer and electronic circuit communication in the next section.

The transmitted and received signals shown in Figure 6 are used to compare with similar signals in [48]. Our achieved result is better than the achievement of secure communication in [48].

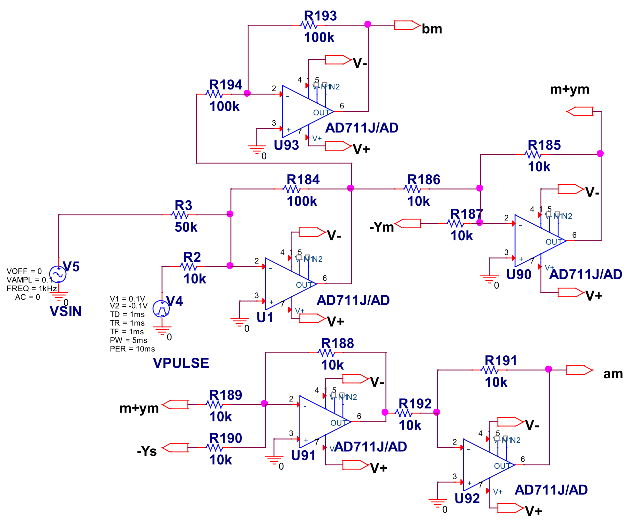

FIGURE 23. Data secure scheme.

B. EXEPERIMENTAL BASIC FOR SYNCHRONIZATION AND ITS APPLICATION TO TWO LORENZ SYSTEMS: THE COMPUTER COMMUNICATION APPROACH

The experimental setup is shown in Figure 8 below. The computer configurations are an Intel(R) Core(TM) i7-2600 CPU @ 3.40 GHz, 4.00 GB RAM for the master and an Intel(R) Core(TM) i7-2600 CPU @ 3.40 GHz, 10.0 GB RAM for the slave system. Both of these computers use the 64-bit of Windows 10. The output signals of the computers communication experiment are shown in Figure 9 below. The parameters of controller and observer for computer communication were selected to be the same as the communication parameters in the simulation section.

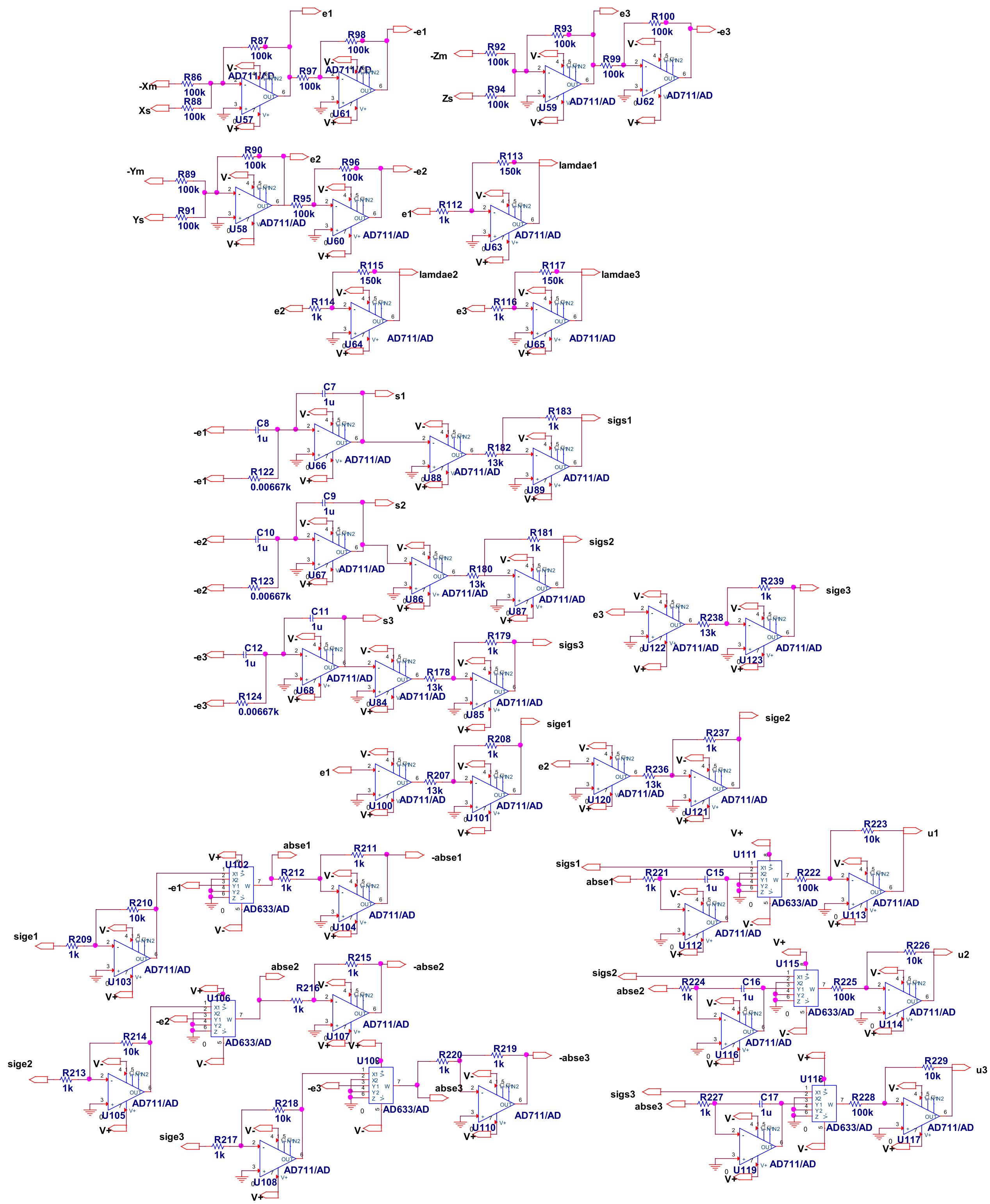

FIGURE 24. Adaptive fuzzy sliding mode control for secure communication system.

The master and slave system state error is calculated as following Figure 10 below. The master and slave system states precisely track each other. The tracking error values are $e_1 \in [-4.13 \cdot 10^{-3}; 3.29 \cdot 10^{-3}]$, $e_2 \in [-3.74 \cdot 10^{-3}; 4.34 \cdot 10^{-3}]$ and $e_3 \in [-7.20 \cdot 10^{-3}; 5.96 \cdot 10^{-3}]$ for the synchronization error on the x-, y-, and z-axis, respectively. The maximum reaching times is approximately 0.03 second, and there are no overshoot values. The disturbance observer response signals

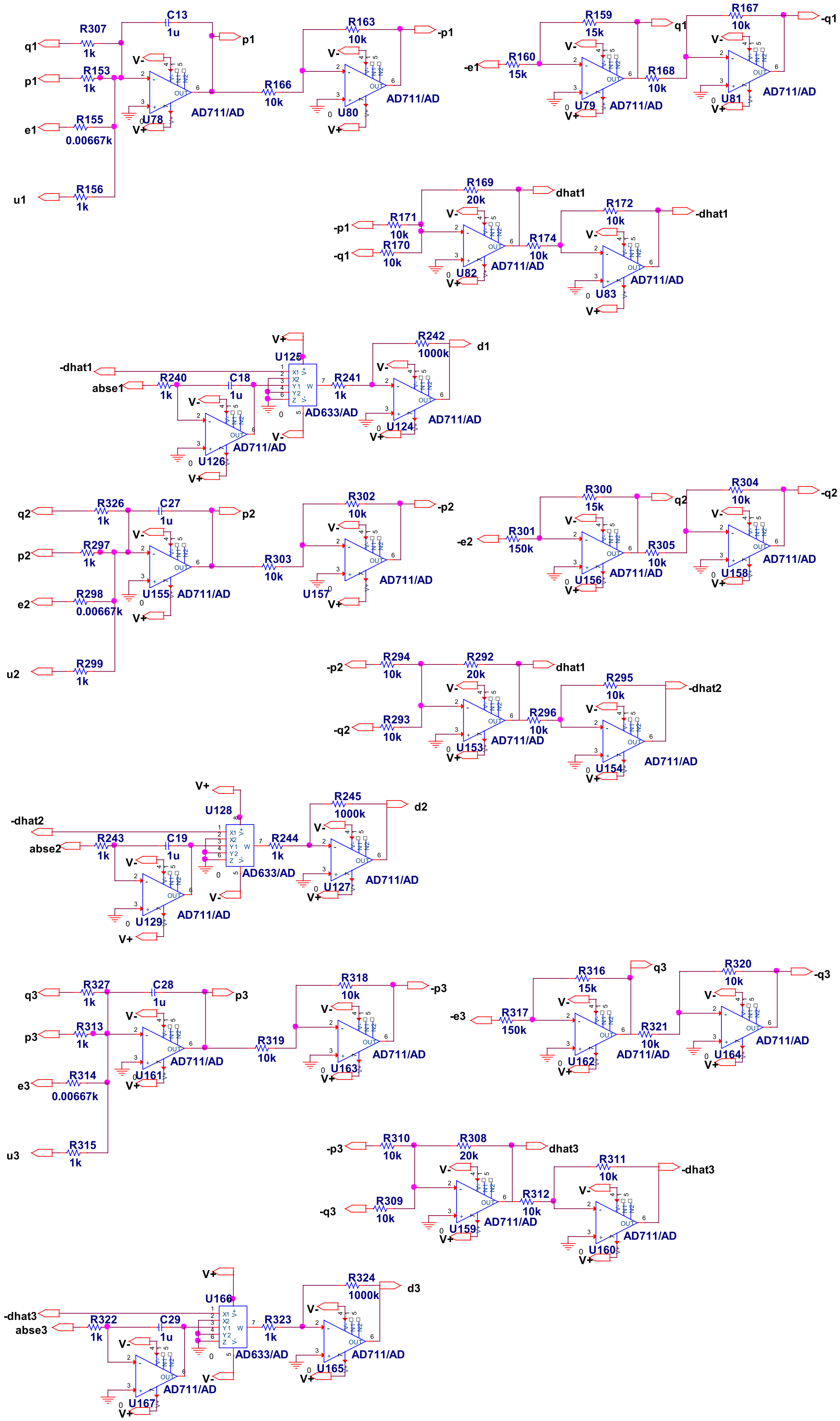

FIGURE 25. Adaptive fuzzy disturbance observer for secure communication system.

are shown as The compensation values of disturbance and uncertainty can be calculated precisely with highly adaptive gains. The y-axis states of master and slave are used to encrypt and decrypt the signal. The sent and received signals are shown in Figure 12 below.

The sent and received signals on the master and slave systems are mostly equal. For more detail about our proposed control algorithm effectiveness, the proposed control methods can be applied to electronic circuits in the next section.

C. SYNCHRONIZATION AND ITS APPLICATION OF TWO LORENZ CHAOTIC SYSTEMS BASED ON EXPERIMENTS: AN ELECTRONIC CIRCUIT' COMMUNICATION APPROACH

This section presents the secure communication of chaotic Lorenz systems based on the electronic circuit. The experimental setup is shown in Figure 13. where the initial conditions of master and slave systems are determined by the capacitor and resistor values. Details are given in the Figures in the Appendix section. The general chaotic Lorenz system is shown as Figure 19 in the Appendix. The experimental electrical voltage was supplied by a GWINSTEK GPC-6030-D Dual tracking with a machine fixed at 5 V. The measurement device is a Tektronix DPO 2014B digital phosphor oscilloscope. The Lorenz system characteristics are shown in Figure 14 below.

The system phase trajectories of the actual experiment are quite similar to the simulation in MATLAB software.

The control gains were selected as follows:

$$\lambda = \begin{bmatrix} 150 & 0 & 0 \\ 0 & 150 & 0 \\ 0 & 0 & 150 \end{bmatrix}, k_0 = \begin{bmatrix} 0.01 & 0 & 0 \\ 0 & 0.01 & 0 \\ 0 & 0 & 0.01 \end{bmatrix},$$
$$L_d = \begin{bmatrix} 1 & 0 & 0 \\ 0 & 0.1 & 0 \\ 0 & 0 & 0.1 \end{bmatrix}, \text{ and } \alpha_0 = \begin{bmatrix} 100 & 0 & 0 \\ 0 & 100 & 0 \\ 0 & 0 & 100 \end{bmatrix}.$$

The Lorenz system characteristics are shown. The synchronized given output of two Lorenz chaotic systems in the electronic circuit experiment is obtained as follows:

The synchronization between two nonidentical Lorenz systems was successfully achieved. The system states error values are very small, that is $e_1 \in [-200 \text{ mV}; 180 \text{ mV}]$, $e_2 \in [-200 \text{ mV}; 220 \text{ mV}]$, and $e_3 \in [-220 \text{ mV}; 220 \text{ mV}]$ for master and slave synchronization error on the x-, y-, and z-axis, respectively. The synchronization maximum tracking error is about 2%. To obtain the above desired goals, the adaptive fuzzy sliding mode and disturbance observer were constructed together in the synchronization system. The actual circuit implementation always contains disturbance and uncertainty due to the changing of the main capacitors, resistors, and of the parasite capacitor, resistor values on the main circuit boards. There is a need to improve disturbance and uncertainty estimation to improve the performance of the synchronization method. The system' perturbations are shown in Figure 16 below.

The synchronization result is the backbone of the data secure communication system. The secure communication given in Eq. (14) can be used to transfer data from the master to slave system areas by following Figure 17.

The secret data transmission from master system to slave with 40 (m) distance can be obtained very precisely after encryption and decryption. The secure communication is executed by the adaptive fuzzy disturbance observer and adaptive fuzzy sliding-mode control. The sent data and received data are shown in Figure 18 below.

The sent and received signals are mostly identical.

V. CONCLUSION

This paper presented synthetic adaptive fuzzy sliding-mode control and a disturbance observer to synchronize two non-identical Lorenz systems, which was taken advantage of to communicate securely across a distance of 40 m between master and slave system in electronic circuits experiments. The adaptive fuzzy sliding-mode control and adaptive disturbance observer were completely constructed based on T-S fuzzy systems. The adaptive law was simply defined by integrating the system state tracking error value. The synchronization tracking error values of the master and slave systems are quite small, with an imprecision of approximately 2% for implementation of the electronic circuits, in which the display devices may be main cause of imprecision. Furthermore, the disturbance and uncertainty of the master and slave systems were perfectly deleted by a new adaptive fuzzy disturbance observer. The simulation of MATLAB and communication of computers were used to show the effectiveness of the disturbance observer. The computer and electronic circuit implementations were utilized to verify that the proposed synchronization control algorithms are necessary for secure data transmission. This suggests our future work on actual data transmission, where the electronic components are key points and the adaptive symmetry phenomenon can be considered.

APPENDIX

See Figures 19–25.

REFERENCES

[1] Y.-J. Chen, H.-G. Chou, W.-J. Wang, S.-H. Tsai, K. Tanaka, H. O. Wang, and K.-C. Wang, "A polynomial-fuzzy-model-based synchronization methodology for the multi-scroll Chen chaotic secure communication system," *Eng. Appl. Artif. Intell.*, vol. 87, Jan. 2020, Art. no. 103251.

[2] S. Çiçek, U. E. Kocamaz, and Y. Uyaroğlu, "Secure communication with a chaotic system owning logic element," *AEU-Int. J. Electron. Commun.*, vol. 88, pp. 52–62, May 2018.

[3] H. Delavari and M. Mohadeszadeh, "Robust finite-time synchronization of non-identical fractional-order hyperchaotic systems and its application in secure communication," *IEEE/CAA J. Automatica Sinica*, vol. 6, no. 1, pp. 228–235, Jan. 2019.

[4] B. Vaseghi, M. A. Pourmina, and S. Mobayen, "Secure communication in wireless sensor networks based on chaos synchronization using adaptive sliding mode control," *Nonlinear Dyn.*, vol. 89, no. 3, pp. 1689–1704, Aug. 2017.

[5] M. H. Abd, F. R. Tahir, G. A. Al-Suhail, and V.-T. Pham, "An adaptive observer synchronization using chaotic time-delay system for secure communication," *Nonlinear Dyn.*, vol. 90, no. 4, pp. 2583–2598, Dec. 2017.

[6] D. Chang, Z. Li, M. Wang, and Y. Zeng, "A novel digital programmable multi-scroll chaotic system and its application in FPGA-based audio secure communication," *AEU-Int. J. Electron. Commun.*, vol. 88, pp. 20–29, May 2018.

[7] Y. Wang, H. R. Karimi, and H. Yan, "An adaptive event-triggered synchronization approach for chaotic Lur'e systems subject to aperiodic sampled data," *IEEE Trans. Circuits Syst. II, Exp. Briefs*, vol. 66, no. 3, pp. 442–446, Mar. 2019.

[8] T. Wang, D. Wang, and K. Wu, "Chaotic adaptive synchronization control and application in chaotic secure communication for industrial Internet of Things," *IEEE Access*, vol. 6, pp. 8584–8590, 2018.

[9] G. Wen, Y. Wan, J. Cao, T. Huang, and W. Yu, "Master–slave synchronization of heterogeneous systems under scheduling communication," *IEEE Trans. Syst., Man, Cybern., Syst.*, vol. 48, no. 3, pp. 473–484, Mar. 2018.

[10] J. Sun, Y. Wu, G. Cui, and Y. Wang, "Finite-time real combination synchronization of three complex-variable chaotic systems with unknown parameters via sliding mode control," *Nonlinear Dyn.*, vol. 88, no. 3, pp. 1677–1690, May 2017.

[11] L. Zhou and F. Tan, "A chaotic secure communication scheme based on synchronization of double-layered and multiple complex networks," *Nonlinear Dyn.*, vol. 96, no. 2, pp. 869–883, Apr. 2019.

[12] L. Zhou, F. Tan, F. Yu, and W. Liu, "Cluster synchronization of two-layer nonlinearly coupled multiplex networks with multi-links and time-delays," *Neurocomputing*, vol. 359, pp. 264–275, Sep. 2019.

[13] H. Lin, C. Wang, and Y. Tan, "Hidden extreme multistability with hyperchaos and transient chaos in a Hopfield neural network affected by electromagnetic radiation," *Nonlinear Dyn.*, vol. 99, no. 3, pp. 2369–2386, Feb. 2020.

[14] A. D. Pano-Azucena, J. de Jesus Rangel-Magdaleno, E. Tlelo-Cuautle, and A. de Jesus Quintas-Valles, "Arduino-based chaotic secure communication system using multi-directional multi-scroll chaotic oscillators," *Nonlinear Dyn.*, vol. 87, no. 4, pp. 2203–2217, Mar. 2017.

[15] X. Song, J. Man, S. Song, and C. K. Ahn, "Gain-scheduled finite-time synchronization for reaction-diffusion memristive neural networks subject to inconsistent Markov chains," *IEEE Trans. Neural Netw. Learn. Syst.*, early access, Jul. 31, 2020, doi: 10.1109/TNNLS.2020.3009081.

[16] X. N. Song, J. T. Man, S. Song, and C. K. Ahn, "Finite/fixed-time antisynchronization of inconsistent Markovian quaternion-valued memristive neural networks with reaction-diffusion terms," *IEEE Trans. Circuits Syst. I, Reg. Papers*, vol. 68, no. 1, pp. 363–375, Jan. 2021.

[17] C. S. Pappu, B. C. Flores, P. S. Debroux, and J. E. Boehm, "An electronic implementation of Lorenz chaotic oscillator synchronization for bistatic radar applications," *IEEE Trans. Aerosp. Electron. Syst.*, vol. 53, no. 4, pp. 2001–2013, Mar. 2017.

[18] S. Yang, C. Li, and T. Huang, "Synchronization of coupled memristive chaotic circuits via state-dependent impulsive control," *Nonlinear Dyn.*, vol. 88, no. 1, pp. 115–129, Apr. 2017.

[19] M. Kountchou, P. Louodop, S. Bowong, H. Fotsin, and Saïdou, "Analog circuit design and optimal synchronization of a modified Rayleigh system," *Nonlinear Dyn.*, vol. 85, no. 1, pp. 399–414, Mar. 2016.

[20] C. Li, F. Min, and C. Li, "Multiple coexisting attractors of the serial–parallel memristor-based chaotic system and its adaptive generalized synchronization," *Nonlinear Dyn.*, vol. 94, no. 4, pp. 2785–2806, Dec. 2018.

[21] T. Karimov, D. Butusov, V. Andreev, A. Karimov, and A. Tutueva, "Accurate synchronization of digital and analog chaotic systems by parameters re-identification," *Electron.*, vol. 7, no. 123, pp. 1–10, Jul. 2018.

[22] D. N. Butusov, T. I. Karimov, I. A. Lizunova, A. A. Soldatkina, and E. N. Popova, "Synchronization of analog and discrete Rössler chaotic systems," in *Proc. IEEE Conf. Russian Young Researchers Electr. Electron. Eng. (EIConRus)*, St. Petersburg, Russia, Feb. 2017, pp. 265–270.

[23] V. Nam Giap, S.-C. Huang, Q. Dich Nguyen, and T.-J. Su, "Disturbance observer-based linear matrix inequality for the synchronization of Takagi-Sugeno fuzzy chaotic systems," *IEEE Access*, vol. 8, pp. 225805–225821, Dec. 2020.

[24] T. Takagi and M. Sugeno, "Fuzzy identification of systems and its applications to modeling and control," *IEEE Trans. Syst., Man, Cybern.*, vols. SMC–15, no. 1, pp. 116–132, Jan. 1985.

[25] K. Tanaka and H. Wang, *Fuzzy Control Systems Design and Analysis: A Linear Matrix Inequality Approach*. New York, NY, USA: Wiley, 2001.

[26] J. H. Kim, C. H. Hyun, E. Kim, and M. Park, "Adaptive synchronization of uncertain chaotic systems based on T-S fuzzy model," *IEEE Trans. Fuzzy Syst.*, vol. 15, no. 3, pp. 69–359, Jun. 2007.

[27] H. S. Kim, J. B. Park, and Y. H. Joo, "Fuzzy-model-based sampled-data chaotic synchronisation under the input constraints consideration," *IET Control Theory Appl.*, vol. 13, no. 2, pp. 288–296, Jan. 2019.

[28] H. K. Lam, W. K. Ling, H. H. Iu, and S. S. Ling, "Synchronization of chaotic systems using time-delayed fuzzy state-feedback controller," *IEEE Trans. Circuits Syst. I, Reg. Papers*, vol. 55, no. 3, pp. 893–903, May 2008.

[29] Y. Zhao, B. Li, J. Qin, H. Gao, and H. R. Karimi, "H_∞ consensus and synchronization of nonlinear systems based on a novel fuzzy model," *IEEE Trans. Cybern.*, vol. 43, no. 6, pp. 2157–2169, Dec. 2013.

[30] J.-H. Kim, C.-H. Hyun, E. Kim, and M. Park, "Adaptive synchronization of uncertain chaotic systems based on T–S fuzzy model," *IEEE Trans. Fuzzy Syst.*, vol. 15, no. 3, pp. 359–369, Jun. 2007.

[31] R. Wang, B. Li, Z. Zhao, J. Guo, and Z. Zhu, "Synchronization of fuzzy control design based on Bessel-Legendre inequality for coronary artery state time-delay system," *IEEE Access*, vol. 7, pp. 1941–181933, Dec. 2019.

[32] R. Sakthivel, R. Sakthivel, O. Kwon, and P. Selvaraj, "Synchronisation of stochastic T–S fuzzy multi-weighted complex dynamical networks with actuator fault and input saturation," *IET Control Theory Appl.*, vol. 14, no. 14, pp. 1957–1967, Sep. 2020.

[33] E. N. Lorenz, "Deterministic nonperiodic flow," *J. Atmos. Sci.*, vol. 20, no. 2, pp. 130–141, Mar. 1963.

[34] K. M. Cuomo, A. V. Oppenheim, and S. H. Strogatz, "Synchronization of Lorenz-based chaotic circuits with applications to communications," *IEEE Trans. Circuits Syst. II, Analog Digit. Signal Process.*, vol. 40, no. 10, pp. 626–633, Oct. 1993.

[35] T.-L. Liao and N.-S. Huang, "An observer-based approach for chaotic synchronization with applications to secure communications," *IEEE Trans. Circuits Syst. I, Fundam. Theory Appl.*, vol. 46, no. 9, pp. 1144–1150, Sep. 1999.

[36] I. N'Doye, H. Voos, and M. Darouach, "Observer-based approach for fractional-order chaotic synchronization and secure communication," *IEEE J. Emerg. Sel. Topics Circuits Syst.*, vol. 3, no. 3, pp. 442–450, Sep. 2013.

[37] P. Selvaraj, R. Sakthivel, and H. Reza Karimi, "Equivalent-input-disturbance-based repetitive tracking control for Takagi–Sugeno fuzzy systems with saturating actuator," *IET Control Theory Appl.*, vol. 10, no. 15, pp. 1916–1927, Oct. 2016.

[38] R. Sakthivel, S. Harshavarthini, R. Kavikumar, and Y.-K. Ma, "Robust tracking control for fuzzy Markovian jump systems with time-varying delay and disturbances," *IEEE Access*, vol. 6, pp. 66861–66869, 2018.

[39] S. Hwang and H. S. Kim, "Extended disturbance observer-based integral sliding mode control for nonlinear system via T–S fuzzy model," *IEEE Access*, vol. 8, pp. 116090–116105, Jun. 2020.

[40] W.-H. Chen, "Disturbance observer based control for nonlinear systems," *IEEE/ASME Trans. Mechatronics*, vol. 9, no. 4, pp. 706–710, Dec. 2004.

[41] A. T. Nguyen, B. A. Basit, H. H. Choi, and J.-W. Jung, "Disturbance attenuation for surface-mounted PMSM drives using nonlinear disturbance observer-based sliding mode control," *IEEE Access*, vol. 8, pp. 86345–86356, May 2020.

[42] X. Wu, K. Xu, M. Lei, and X. He, "Disturbance-compensation-based continuous sliding mode control for overhead cranes with disturbances," *IEEE Trans. Autom. Sci. Eng.*, vol. 17, no. 4, pp. 2182–2189, Oct. 2020.

[43] X. Liu, H. Yu, J. Yu, and Y. Zhao, "A novel speed control method based on port-controlled Hamiltonian and disturbance observer for PMSM drives," *IEEE Access*, vol. 7, pp. 111115–111123, 2019.

[44] V. Utkin, "Variable structure systems with sliding modes," *IEEE Trans. Autom. Control*, vol. AC-22, no. 2, pp. 212–222, Apr. 1977.

[45] C. C. Fuh, "Variable-thickness boundary layers for sliding mode contro," *J. Mar. Sci. Tech.*, vol. 16, no. 4, pp. 288–294, Dec. 2008.

[46] V.-N. Giap and S.-C. Huang, "Effectiveness of fuzzy sliding mode control boundary layer based on uncertainty and disturbance compensator on suspension active magnetic bearing system," *Meas. Control*, vol. 53, nos. 5–6, pp. 934–942, Mar. 2020.

[47] G. Gandikota and D. K. Das, "Disturbance observer–based adaptive boundary layer sliding mode controller for a type of nonlinear multiple-input multiple-output system," *Int. J. Robust Nonlinear Control*, vol. 29, no. 17, pp. 5886–5912, Aug. 2019.

[48] V. H. P. Rodrigues, T. R. Oliveira, and J. P. V. S. Cunha, "Globally stable synchronization of chaotic systems based on norm observers connected in cascade," *IEEE Trans. Circuits Syst. II, Exp. Briefs*, vol. 63, no. 9, pp. 883–887, Sep. 2016.

VAN NAM GIAP received the B.S. degree in control engineering and automation from the Hanoi University of Science and Technology, Hanoi, Vietnam, in 2015, and the master's degree in electronic engineering from the National Kaohsiung University of Applied and Sciences, Kaohsiung, Taiwan, in 2017. He is currently pursuing the Ph.D. degree in mechanical engineering with the National Kaohsiung University of Science and Technology, Taiwan. His research interests include sliding mode control, disturbance and uncertainty estimation, fuzzy logic control, and the magnetic bearing systems and its applications.

QUANG DICH NGUYEN received the B.S. degree in electrical engineering from the Hanoi University of Technology, Hanoi, Vietnam, in 1997, the M.S. degree in electrical engineering from the Dresden University of Technology, Dresden, Germany, and the Ph.D. degree from Ritsumeikan University, Kusatsu, Japan, in 2003 and 2010, respectively. Since 2000, he has been with the Hanoi University of Science and Technology, Vietnam, where he is currently an Associate Professor and the Executive Dean of the Institute for Control Engineering and Automation. His research interests include magnetic bearings, self-bearing motors, and sensorless motor control.

SHYH-CHOUR HUANG (Senior Member, IEEE) received the bachelor's degree in aeronautics and astronautics engineering from National Cheng-Kung University, in 1980, Taiwan, and the Ph.D. degree in mechanical engineering from the University of Cincinnati, USA, in 1990. He is currently a Professor of Mechanical Engineering with the National Kaohsiung University of Science and Technology, Taiwan. His research interests include micro-electromechanical systems' design, biomechanics, compliant mechanisms, multibody dynamics, fuzzy logic control, vibration control, and optimization algorithms.